

1
2
3
4
5
6
7
8
9
10
11
12
13
14
15
16
17
18
19
20
21
22
23
24
25
26
27
28

MS. LILLIAN D. PARKER (Orcid ID : 0000-0003-3370-9473)
DR. MIGUEL CAMACHO-SANCHEZ (Orcid ID : 0000-0002-6385-7963)
DR. MICHAEL G. CAMPANA (Orcid ID : 0000-0003-0461-6462)
DR. JENNIFER LEONARD (Orcid ID : 0000-0003-0291-7819)

Article type : Original Article

Little genetic structure in a Bornean endemic small mammal across a steep ecological gradient

Running title: Gene flow across elevations in *Tupaia montana*

Lillian D. Parker^{1,3†*}, Melissa T.R. Hawkins^{1,2,4†}, Miguel Camacho-Sanchez⁵, Michael G. Campana^{1,3,4}, Jacob A. West-Roberts^{1,6}, Tammy R. Wilbert¹, Haw Chuan Lim², Larry L. Rockwood², Jennifer A. Leonard⁵ & Jesús E. Maldonado^{1,3,4}

†these authors should be considered joint first author

* Corresponding author (parkerld@si.edu)

Affiliations

¹Center for Conservation Genomics, Smithsonian Conservation Biology Institute and National Zoological Park, Washington DC, USA; ²Division of Mammals, Department of Vertebrate Zoology, National Museum of Natural History, Smithsonian Institution, Washington, DC, USA; ³School of Systems Biology and ⁴Department of Environmental Science and Policy, George Mason University, Fairfax, Virginia, USA; ⁵Conservation and Evolutionary Genetics Group,

This is the author manuscript accepted for publication and has undergone full peer review but has not been through the copyediting, typesetting, pagination and proofreading process, which may lead to differences between this version and the [Version of Record](#). Please cite this article as [doi: 10.1111/MEC.15626](https://doi.org/10.1111/MEC.15626)

This article is protected by copyright. All rights reserved

29 Estación Biológica de Doñana (EBD-CSIC), Seville, Spain; ⁶Department of Computational
30 Biology, Carnegie Mellon University, Pittsburgh, Pennsylvania, USA

31
32
33
34
35
36
37
38
39
40
41
42
43
44
45
46
47
48
49
50
51
52
53
54
55
56
57
58

Abstract

Janzen’s influential “mountain passes are higher in the tropics” hypothesis predicts restricted gene flow and genetic isolation among populations spanning elevational gradients in the tropics. Few studies have tested this prediction, and studies that focus on population genetic structure in Southeast Asia are particularly underrepresented in the literature. Here, we test the hypothesis that mountain treeshrews (*Tupaia montana*) exhibit limited dispersal across their broad elevational range which spans ca. 2300 meters on two peaks in Kinabalu National Park (KNP) in Borneo: Mt. Tambuyukon (MT) and Mt. Kinabalu (MK). We sampled 83 individuals across elevations on both peaks and performed population genomics analyses on mitogenomes and SNPs from 4,106 ultraconserved element loci. We detected weak genetic structure and infer gene flow both across elevations and between peaks. We found higher genetic differentiation on MT than MK despite its lower elevation and associated environmental variation. This implies that, contrary to our hypothesis, genetic structure in this system is not primarily shaped by elevation. We propose that this pattern may instead be the result of historical processes and limited upslope gene flow on MT. Importantly, our results serve as a foundational estimate of genetic diversity and population structure from which to track potential future effects of climate change on mountain treeshrews in KNP, an important conservation stronghold for the mountain treeshrew and other montane species.

Keywords: elevational range, mountain treeshrews, conservation genetics, population genomics, ultraconserved elements, mitogenomes

59
60
61
62
63
64
65
66
67
68
69
70
71
72
73
74
75
76
77
78
79
80
81
82
83
84
85
86
87
88

Introduction

Tropical ecosystems are global hotspots of biodiversity and endemism. To explain the higher diversity in lower latitude regions, Janzen (1967) proposed that the greater temporal thermal stability and spatial environmental heterogeneity on tropical mountains should select for narrow thermal tolerances which in turn reduce effective dispersal and increase population isolation across elevational gradients (Ghalambor, Huey, Martin, Tewksbury, & Wang, 2006; Gill et al., 2016). Numerous studies support the first prediction of the hypothesis that species in the tropics have narrower elevational ranges than those in the temperate zone (Ghalambor et al., 2006; McCain, 2009). Fewer studies have tested the second prediction that restricted gene flow among populations spanning elevational gradients results in genetic divergence (Ghalambor et al., 2006). Available data regarding this prediction are contradictory: some studies have found significant population genetic divergence across elevations, for example, in insects (Gueuning et al., 2017; Polato et al., 2018) and in endotherms including birds (Bertrand et al., 2014; DuBay & Witt, 2014; Gadek et al., 2018; Linck, Freeman, & Dumbacher, 2019) and mammals (Feijó et al., 2019). Others detected high rates of gene flow alongside adaptive phenotypic divergence (Branch, Jahner, Kozlovsky, Parchman, & Pravosudov, 2017; Cheviron & Brumfield, 2009).

Few studies have investigated the spatial population genetic structure of small mammals across elevational gradients in tropical montane ecosystems (Muenchow, Dieker, Kluge, Kessler, & von Wehrden, 2018). Thus, the influence of elevational gradients on gene flow in terrestrial endotherms at small spatial scales is not well understood. Studying spatial population genetic structure in the montane tropics is important not only because it allows for hypothesis testing regarding the effects of elevational gradients on genetic structure, but also because it enables researchers to identify distinct evolutionary units warranting protection and to establish benchmarks from which to monitor responses to changing global environmental conditions (Camacho-Sanchez et al. 2018; Castillo Vardaro, Epps, Frable, & Ray, 2018; Moritz, 1994). This is critical given the vulnerability of tropical montane ecosystems to the impacts of global climate

89 change (GCC) (Feeley, Stroud, & Perez, 2017; Lenoir & Svenning, 2015).

90 Here, we investigate the genetic structure of the mountain treeshrew, *Tupaia montana*,
91 across its full elevational range on two mountains in Kinabalu National Park (KNP), Sabah,
92 Borneo: Mt. Kinabalu (MK) and Mt. Tambuyukon (MT) (Figure 1). The mountain treeshrew
93 provides an interesting system in which to study the effect of environmental gradients on
94 population structure because it has a broad elevational distribution compared to other small
95 mammals in KNP (Camacho-Sanchez, Hawkins, Tuh Yit Yu, Maldonado, & Leonard, 2019;
96 Nor, 2001). On MK, the species occurs from ca. 900 meters above sea level (masl) to at least
97 3200 masl, encompassing four vegetation zones; on MT it ranges from ca. 900 meters to the
98 summit at 2,579 masl, including three vegetation zones (Kitayama, 1992). Given the temperature
99 lapse rate in KNP at -0.55°C per 100 meters of elevation gain (Kitayama, 1992), mountain
100 treeshrews experience a 12.65°C average range in temperature on MK, which is higher than the
101 thermal neutral zone for most small mammals (Khaliq, Hof, Prinzinger, Böhning-Gaese, &
102 Pfenninger, 2014). On MT, mountain treeshrews experience an 8.8°C temperature range
103 (Camacho-Sanchez et al., 2018).

104 Mountain treeshrews exhibit facultative mutualism with pitcher plants in the genus
105 *Nepenthes* – treeshrews consume the plants' carbohydrate-rich secretions and defecate into the
106 pitchers, providing the plants supplementary nitrogen and phosphorous (Chin, Moran, & Clarke,
107 2010; Clarke et al., 2009). Although mountain treeshrews provide critical nutrients to the plant,
108 the importance of the plant to treeshrews is unknown. The range of mountain treeshrews exceeds
109 that of the plants - none of the plants are distributed below 1200 masl or above 2650 masl. As
110 such, treeshrews are not reliant on them for nutrients even in high elevations areas without
111 fruiting trees.

112 We test the hypothesis that, consistent with Janzen's (1967) hypothesis, restricted gene
113 flow across the steep ecological gradient that mountain treeshrews inhabit has resulted in
114 significant genetic differentiation. Although the ecology of mountain treeshrews is poorly
115 understood, our hypothesis is informed by observations of small home ranges (Emmons, 2000;
116 Payne, Francis, & Phillipps, 2016) and phenotypic changes associated with elevational changes
117 (Hinckley et al., in review). We predict that mountain treeshrews will exhibit significant
118 differentiation in neutral genetic markers 1) between mountains, due to limited dispersal across

119 the lowland habitat that connects them, and 2) across elevations – with greater differentiation on
120 MK due to its higher elevation and associated environmental variability.

121 To test our predictions, we analyze both mitochondrial genomes (mitogenomes) and
122 nuclear ultraconserved element (UCE)-associated single nucleotide polymorphism (SNP)
123 markers from mountain treeshrews collected across their full elevational range in KNP in a
124 population genetics framework. Previous studies have shown that UCEs are sufficiently variable
125 to resolve shallow phylogenies on a phylogeographic scale, (Faircloth et al., 2012; Harvey,
126 Smith, Glenn, Faircloth, & Brumfield, 2016; Mason, Olvera-Vital, Lovette, & Navarro-
127 Sigüenza, 2018; Smith, Harvey, Faircloth, Glenn, & Brumfield, 2014) including intraspecific
128 phylogenies (Giarla et al., 2018), and to answer questions regarding recently diverged species
129 (Oswald et al., 2016; Winker, Glenn, & Faircloth, 2018). However, ours is one of the first studies
130 to describe the intraspecific variability of SNPs derived from UCE loci at a fine spatial scale.

131

132 **Materials and methods**

133

134 *Sample collection*

135 We trapped small mammals on both MK and MT within KNP (6°09'N 116°39'E) during
136 two field seasons in 2012 and 2013. At 4,095 meters above sea level (masl), MK is the tallest
137 mountain in the Sundaland biogeographic region. It is relatively young, having reached its
138 present height ca. 1 million years ago (Mya) (Hall et al., 2009). Eighteen kilometers to the north
139 of MK, the less-studied MT stands at 2,579 masl (Figure 1a). MT is older - its major uplift
140 occurred as part of a different geological process, as part of the Crocker Range, 7–11 Mya (Hall
141 et al., 2009).

142 Our trapping methodology and permitting information is described in Camacho-Sanchez
143 et al. (2019). Briefly, we set traps from ca. 503 to 3,466 masl on MK and ca. 331 to 2,509 masl
144 on MT and (Figure 1a). The mountain treeshrew was the most frequently caught species,
145 representing 37.5% of all catches. For this study, we included 92 *Tupaia* individuals: 84
146 mountain treeshrews and eight outgroup individuals from three congeners, the pygmy treeshrew

147 (*T. minor*, $n = 2$), the large treeshrew (*T. tana*, $n = 5$), and the ruddy treeshrew (*T. splendidula*, n
148 = 1), the sister species of the mountain treeshrew (Roberts, Lanier, Sargis, & Olson, 2011; Table
149 S1).

150 151 *Laboratory methods*

152 Laboratory work was performed at the Center for Conservation Genomics (CCG),
153 Smithsonian Conservation Biology Institute, Washington, DC. We extracted DNA from liver and
154 ear punch samples using a DNeasy Blood and Tissue Kit (Qiagen, Valencia CA) following the
155 manufacturer's protocol. We amplified whole mitogenomes in two fragments using long range
156 PCR, fragmented the PCR products to an average length of 500 base pairs (bps) using a Qsonica
157 Q800R sonicator (QSonica, Newtown, CT, USA), and prepared single-indexed DNA libraries
158 for sequencing using a Kapa LTP Library Preparation kit (Kapa Biosystems, Wilmington, MA)
159 following Hawkins et al. (2016). We pooled libraries equimolarly and sequenced on an Illumina
160 MiSeq with 2×100 base pair (bp) reads (Illumina, Inc., San Diego, CA).

161 We used in-solution DNA hybridization to enrich genomic DNA for UCEs following
162 Hawkins et al. (2016). We sheared DNA extracts and constructed indexed libraries as above. We
163 quantified libraries using a Qubit® fluorometer (Life Technologies) with a $1 \times$ dsDNA HS assay
164 kit and multiplexed 4-8 samples equimolarly prior to enrichment. We used a NimbleGen SeqCap
165 EZ® kit (Roche, Basel, Switzerland) containing 54,689 unique 60-bp DNA probes representing
166 5,561 vertebrate UCE loci with an average of $4 \times$ tiling per base per locus to enrich multiplexed
167 libraries following the manufacturer's protocol. Post-enrichment libraries were amplified with
168 12–14 cycles of PCR using Kapa HiFi HotStart DNA polymerase (Kapa Biosystems,
169 Wilmington, MA) following the manufacturer's protocol.

170 Following visualization on a Bioanalyzer 2100 (Agilent Technologies, Santa Clara, CA)
171 with High Sensitivity DNA kits, enriched libraries were quantified via qPCR using the Kapa
172 Biosystems Illumina Library Quantification Kit (Kapa Biosystems, Wilmington, MA). Samples
173 were pooled equimolarly and sequenced with 2×150 bp reads on Illumina HiSeq2000 (Semel
174 Institute of Neurosciences, UCLA, & University of Copenhagen, Denmark) and MiSeq® (CCG)
175 platforms.

176

177 *Mitogenome assembly and alignment*

178 We analyzed mitogenomes to investigate the population structure and genetic diversity of
179 mountain treeshrews. Because mitogenomes are inherited matrilineally and are not subject to
180 recombination, they are frequently used to investigate population structure, colonization history,
181 and species' demographic histories (Harrison, 1989).

182 Mitogenome amplicon reads were quality filtered with Trimmomatic v0.33 (Bolger,
183 Lohse, & Usadel 2014) with parameters SLIDINGWINDOW: 4:15 and MINLEN: 36. Since the
184 only publicly available mitogenome representing any *Tupaia* species (the northern treeshrew, *T.*
185 *belangeri* NC_002521; Schmitz, Ohme, & Zischler, 2000) is highly divergent from our study
186 species (Roberts et al., 2011), we first generated reference mitogenomes for the mountain
187 treeshrew and 3 more closely related outgroup species: the pygmy treeshrew, large treeshrew,
188 and ruddy treeshrew. For each species, we selected one individual with the highest number of
189 sequencing reads (pygmy treeshrew, BOR 443; large treeshrew, BOR 010, & ruddy treeshrew,
190 UMMZ174429) and assembled sequences *de novo* with the MIRA v1.0.1 plugin in Geneious
191 v9.1.2 (Biomatters Ltd.), using 'Quality Level Accurate' and default settings. Quality filtered
192 sequence reads were mapped to the appropriate reference using BWA-MEM v0.7.10 (Li 2013)
193 with default parameters. We also assembled mitogenomes from UCE-enriched library sequences
194 (Supplemental Information). Consensus sequences were generated with Geneious (lowest
195 coverage to call a base 5× and Highest Total Quality parameters) and aligned with the MAFFT
196 v7.450 plugin (Kato, Misawa, Kuma, & Miyata. 2002). We transferred annotations from the
197 northern treeshrew reference to the consensus sequences. To rule out the presence of nuclear
198 copies of mitochondrial genes (NUMTs), we translated all protein-coding genes to check for
199 frame shifts or stop codons.

200

201 *Genetic diversity and population structure*

202 Because the inclusion of close relatives can bias estimates of genetic diversity and
203 structure (Goldberg & Waits, 2010), we removed first-order relatives identified by our SNP
204 dataset and performed all subsequent mitogenome analyses with the reduced data (hereafter
205 "unrelated dataset"). We defined haplotypes and calculated haplotype diversity (H_d), nucleotide

206 diversity (π), and Tajima's D using DNAsp v6.12.03 (Librado & Rozas 2009). We estimated the
207 differentiation between MK and MT and between high and low elevations within each peak
208 through analysis of molecular variance (AMOVA) in Arlequin v3.5 (Excoffier & Lischer, 2010)
209 with a permutation test of 10,000 replicates to assess statistical significance. We visualized
210 relationships among haplotypes by generating a median-joining network with PopART v1.7
211 (Leigh & Bryant, 2015).

212

213 *Phylogenetic analysis and modeling demographic history*

214 We performed phylogenetic analyses to place the mitochondrial lineages detected in our
215 mountain treeshrew samples within an evolutionary framework with respect to other Bornean
216 treeshrew species in the *Tupaia* clade (i.e. the large treeshrew, pygmy treeshrew, and ruddy
217 treeshrew), and to confirm the monophyly of the mountain treeshrew within the group. We used
218 PartitionFinder v2.0 (Lanfear, Calcott, Ho, & Guindon, 2012) to select partitions and substitution
219 models and estimated a phylogeny using MrBayes v3.2.6 (Ronquist & Huelsenbeck, 2003). We
220 then used BEAST v.1.8.4 (Drummond & Rambaut, 2007) to estimate the timing of divergence
221 between the mountain treeshrew mitochondrial lineages we identified.

222 To infer demographic history, we performed a Bayesian coalescent skyline plot analysis
223 using BEAST v2.0 (Bouckaert et al., 2014). We used a time to most recent common ancestor
224 (TMRCA) prior of 450,000 years before present (lognormal distribution, $\mu = 0.45$, $\sigma = 0.2$), the
225 estimated date of divergence between the two mitochondrial lineages as determined by the dating
226 analysis performed in BEAST (Supplemental Information).

227

228 *Genotyping UCE-associated SNPs*

229 To generate the SNP dataset, we followed the PHYLUCe v.1.5.0 pipeline with default
230 parameters (Faircloth, 2016) for sequence trimming, *de novo* assembly of contigs, identification
231 of UCE loci, and sequence alignment. We generated a pseudo-genomic reference by aligning
232 each locus with MAFFT v7.407 and trimming using Gblocks v0.91b with default parameters
233 (Castresana, 2000). We then used Geneious to generate a consensus sequence for each locus,
234 replacing ambiguity codes with an appropriate nucleotide at random. We used Picard v1.106
235 (<http://broadinstitute.github.io/picard/>), and SAMtools v1.9 (Li et al., 2009) to create sequence

236 dictionaries and reference indices from the reference. We used the PHYLUCEScript *snps.py* to
237 automate alignment of trimmed reads from each sample to the reference with BWA-MEM
238 v0.7.17, and then called SNPs with the HaplotypeCaller tool of the Genome Analysis Toolkit
239 v3.7 (McKenna et al., 2010) following Giarla and Esselstyn (2015). Using VCFtools v0.1.16
240 (Danecek et al., 2011), we removed SNPs that failed to pass GATK quality filters (QD < 2.0 ||
241 FS > 60.0 || MQ < 40.0 || HaplotypeScore > 13.0 || MappingQualityRankSum < -12.5 ||
242 ReadPosRankSum < -8.0), and selected SNPs with a minimum depth of coverage of 8 per
243 individual and a minor allele frequency $\geq 5\%$. We used *HD_plot.py* (McKinney, Waples, Seeb,
244 & Seeb, 2017) to filter SNPs resulting from putative paralogs or wrongly assembled contigs from
245 the dataset by removing SNPs with heterozygosity > 0.75 and a read-ratio deviation score $D > 10$.
246 The D statistic is a measure of deviation from the expected allelic read ratio of 1:1 when reads
247 are summed over all heterozygous individuals. This method more accurately identifies true SNP
248 loci than methods relying on read depth or heterozygote excess alone (McKinney et al., 2017).
249 After filtering with *HD_plot.py*, we further filtered SNPs that were out of Hardy-Weinberg
250 Equilibrium (HWE) after Bonferroni correction for multiple comparisons ($p < 10^{-5}$) using
251 VCFtools v0.1.16 because strong deviations from HWE are usually indicative of genotyping
252 error (Chen, Cole, & Grong-Ginsbach, 2017). To generate a set of unlinked SNPs, we selected
253 one SNP per UCE using VCFtools v0.1.16 '-thin 2000'. We used the unlinked SNP dataset with
254 10% missing data for all SNP-based analyses except calculation of genetic diversity and
255 effective population size, Principal Components Analysis (PCA), Discriminant Analysis of
256 Principal Components (DAPC) and Bayesian cluster analysis with STRUCTURE v2.3.4
257 (Pritchard, Stephens, & Donnelly, 2000), for which we used a dataset with no missing data.

258

259 *Generating phased pseudo-haplotype sequences*

260 In order to include multiple SNPs per UCE locus as well as invariant sites for the
261 MIGRATE-N analysis, we generated multiple sequence alignments of pseudo-haplotypes. We
262 did this by using the EMIT_ALL_SITES output mode of the GATK HaplotypeCaller tool. We
263 filtered the resulting VCF file to include only UCE loci with at least one SNP with no more than
264 10% missing data. We then generated alignments from the VCF file with a custom Ruby script,
265 *vcf2aln* v0.4.2 (<https://github.com/campanam/vcf2aln>, Supplemental Information). This script

266 utilizes phasing information where present and randomly selects an allele where phase is
267 unresolved.

268 We trimmed the phased UCE sequence alignments with Gblocks v.0.91b (Castresana,
269 2000) using default parameters and quantified informative sites with the
270 *phyluce_align_get_informative_sites.py* PHYLUCEScript. For the final dataset used in the
271 MIGRATE-N analysis, we retained only loci with at least one and fewer than 10 parsimony
272 informative sites (PIS) in order to increase the signal-to-noise ratio of our dataset. MIGRATE-N
273 calculates model and parameter likelihoods for each locus independently and averages results
274 across loci taking into account the posterior distributions of each (Beerli & Palczewski, 2010).
275 Uninformative loci with flat posterior distributions contribute less to the final average; therefore,
276 removing invariant loci should not bias our results, while including them increases computation
277 time. We removed loci with more than 10 PIS, i.e. more than ca. two standard deviations above
278 the mean ($\bar{x} = 3.6$, $SD = 4$) because their diversity is likely artificially high due to errors
279 introduced during *de novo* assembly or sequence alignment (Gilbert, Wu, Simon, Sinsheimer, &
280 Alfaro, 2018). Gilbert et al. (2018) showed that filtering sites on the basis of signal-to-noise in a
281 concatenated UCE alignment improved the resolution of hard-to-resolve nodes in the Neoaves
282 phylogeny, and that after filtration, the topology converged on that derived from a much larger
283 dataset.

284
285 *Genetic diversity and effective population size*

286 We removed individuals that were identified as first-degree relatives (parent-offspring or
287 full siblings) according to the KING v2.1.4 software (Manichaikul et al., 2010), i.e. those with
288 kinship coefficients ≥ 0.18 . Using the unlinked SNPs with 10% missing data, we first calculated
289 pairwise kinship values and identified putative family groups with the KING software and then
290 ran a PC-AiR analysis with GENESIS v2.2.2 (Conomos, Reiner, Weir & Thornton, 2016) in R
291 v3.6.3 (R Core Team 2019, applies to all subsequent use of R) to identify an “unrelated” subset
292 of individuals. We used GenAlEx v6.503 to estimate the statistical power of the SNP dataset to
293 differentiate individuals by calculating $P_{ID_{sib}}$, the probability of two individuals having identical
294 genotypes assuming siblings are present in the data (Waits, Luikart, & Taberlet, 2001).

295 We calculated average expected and observed heterozygosity (H_e and H_o) and the

296 inbreeding coefficient (F_{IS}) with VCFtools v0.1.16 using our SNPs with no missing data. We
297 also concatenated FASTA alignments of UCE sequence pseudo-haplotypes for all individuals in
298 the unrelated dataset and used the maximum composite likelihood method to calculate nucleotide
299 diversity (π) in MEGA v7.0.26 (Kumar, Stecher, & Tamura, 2016).

300 We estimated effective population sizes (N_e) using the linkage disequilibrium model with
301 random mating (Waples & Do, 2008) implemented in NeEstimator v2.1 (Do et al., 2014). We
302 report estimated N_e values using ‘Lowest Allele Frequency Used’ 5% and 95% confidence
303 intervals generated by the ‘Parametric method’ for unrelated individuals for each population
304 cluster identified by STRUCTURE separately.

305

306 *Population structure*

307 We characterized population genetic structure using the SNP dataset with no missing
308 data. We performed PCA and DAPC with the Adegenet v2.1.1 package (Jombart, 2008) in R.
309 For the DAPC analysis, we first conducted K -means clustering and selected the number of
310 clusters based on the lowest Bayesian Information Criterion (BIC) value. We performed cross-
311 validation to determine the number of PCs to retain by calculating the lowest root mean squared
312 error. We then ran DAPC, retaining 20 PCs and 2 discriminant functions.

313 We used STRUCTURE v2.3.4 to infer the number of population clusters (K) and the
314 proportion of individual membership assigned to each cluster (q_k). We used a burn-in of 500,000
315 steps followed by 1,000,000 recorded steps, tracking the probability of the data given K
316 ($\text{LnP}(D)$) to ensure that we ran the program long enough for the values to stabilize. We used the
317 admixture model, no location priors, and assumed correlated allele frequencies (Falush,
318 Stephens, & Pritchard, 2003). We performed a simulation with K from 1 to 7 with 10 replicates
319 each and identified meaningful K values using the ΔK method (Evanno, Regnaut, & Goutdet,
320 2005) implemented in STRUCTURE HARVESTER v0.6.94 (Earl & vonHoldt, 2012). We
321 combined replicate runs using CLUMPP v1.1.2 (Jakobsson & Rosenberg, 2007).

322 To quantify the levels of differentiation between population clusters identified by
323 STRUCTURE, we performed an AMOVA and calculated pairwise F_{ST} values using the SNP
324 dataset with 10% missing data in GenAlEx v6.5 (Peakall & Smouse, 2012), with 10,000
325 permutations to generate the null distribution. To investigate local spatial genetic structure, we

326 performed a Mantel test using ade4 v1.7 (Dray & Dufour, 2007) in R on both the full and
327 unrelated dataset. We tested for a correlation between pairwise genotypic distance and Euclidean
328 geographic distance with 9,999 permutations to generate the null distribution. We also generated
329 a Mantel correlogram to test for spatial autocorrelation between pairs of treeshrews at different
330 distance classes using GenAlEx. We first calculated pairwise linear geographic and genotypic
331 distances, and then used the 'Spatial' option with 9,999 permutations. We defined 7 distance
332 classes (0.2, 1.0, 2.0, 5.0, 10.0, 15.0, and 18.0 km) based on Sturges's Rule (Sturges, 1926),
333 chosen to ensure sufficient comparisons within each class. Finally, we calculated the average,
334 median, and maximum geographic distances between pairs of individuals in each kinship class
335 corresponding to first, second, third-order, and distant relatives (Table 1) as an additional way to
336 quantify the decay of genetic relatedness with distance. To test for significant differences
337 between the means in each kinship class, we performed a one-way ANOVA in R with a Tukey
338 Honest Significant Differences test and a Bonferroni correction for multiple comparisons
339 (Combs, Puckett, Richardson, Mims, & Munshi-South, 2018).

340

341 *Migration and population models*

342 We used the program MIGRATE-N v3.6 with its Bayesian implementation (Beerli, 2005)
343 to compare support for six different models of population structure and migration (diagrams of
344 hypotheses in Figure 2). We used the phased pseudo-haplotype sequence dataset for this analysis
345 to take advantage of the higher information content in DNA sequences relative to SNPs.
346 Although our workflow may generate chimeric sequences in instances where phase is
347 unresolved, we do not expect that this would affect model selection (Andermann et al., 2018; P.
348 Beerli *pers. comm.*). However, to ensure that phase did not affect model inference, we ran the
349 MIGRATE-N analysis twice with different configurations of variants within haplotypes while
350 maintaining all other settings.

351 We compared models to test our *a priori* hypotheses of significant genetic structure and
352 limited gene flow between MK and MT and between high and low elevations. We also included
353 models of population structure based on the STRUCTURE results in order to compare migration
354 rates and directionality between population clusters. The models included the following: 1)
355 panmixia, 2) four populations (high elevation MK, low elevation MK, low elevation MT and

356 high elevation MT) with bidirectional migration between adjacent pairs, 3) three populations
357 (high elevation MT, low elevation MT and all of MK) with bidirectional migration between
358 adjacent pairs, 4) three populations with migration between all pairs, 5) two populations (high
359 elevation MT separate from all others) with bidirectional migration, and 6) two populations with
360 unidirectional migration from high elevation MT (Figure 2).

361 For model 2, we assigned individuals to populations based on their sampling location:
362 low elevation individuals < 2000 masl, and high elevation ≥ 2000 masl. For models 3, 4, 5, and
363 6, we assigned individuals based on STRUCTURE output for $K = 3$ and $K = 2$, respectively. We
364 randomly selected five individuals from each population cluster ($n = 10$ haplotypes). We did not
365 include all individuals because for coalescent processes, increasing the sample size above this
366 does not necessarily improve accuracy, but substantially increases computation time
367 (Felsenstein, 2005). For each model, we ran two long chains of 20,000,000 steps, sampled every
368 100 steps with 50,000 steps per chain discarded as burn-in, and with four heated chains. To
369 ensure comparability across models, we ran the most complex model first and used the same
370 prior distributions and run parameters for all subsequent models. We assessed chain mixing
371 through acceptance ratios and ESS of parameters and genealogies ($ESS \geq 40$ million). We
372 calculated log Bayes factors (LBF) and model probability using the Bezier approximation of the
373 marginal model likelihood and the formula described in (Beerli & Palczewski, 2010).

374

375 **Results**

376 *DNA Sequencing*

377 We obtained mitochondrial genome sequences from 83 mountain treeshrew individuals
378 (MT423905–MT423940) and 8 sequences from three congeners (MT442045–MT442052): the
379 large treeshrew ($n = 5$), the small treeshrew ($n = 2$), and the ruddy treeshrew ($n = 1$).

380 Mitogenomes were sequenced to an average depth of $50\times$.

381 We sequenced UCEs from 80 mountain treeshrews (SRA accession PRJNA629376).

382 Each UCE-enriched library was sequenced with a mean of 2.3 million reads (914,104–

383 7,011,836), yielding a mean of 3,344 UCE loci (2,137–3,489) per sample. The total number of

384 UCE alignments that we used to generate the pseudo-reference was 4,106, and the mean length

385 was 495 bps (149–2167 bps). After aligning reads to the pseudo-reference and quality filtering,

386 there were 7,861 SNPs including multiple SNPs per locus. After removing loci with more than
387 10% missing data across individuals, 3,168 SNPs remained. The unlinked SNP dataset included
388 1,794 independent SNPs. Removing loci with missing data left 684 unlinked loci. In the phased
389 pseudo-haplotype sequence alignment dataset used for the MIGRATE-N analysis, 1,664 UCE
390 alignments remained after removing loci with less than one (114 loci) and more than 10 PIS (16
391 loci) (Figure S1).

392

393 *Mitogenomes: genetic diversity, population structure, and demographic inference*

394 There were 36 unique mitochondrial haplotypes in the dataset that included close
395 relatives ($n = 83$), and 34 among the 58 unrelated individuals. All subsequent analyses were
396 performed with the unrelated dataset. H_d was high, at 0.977 (SD 0.008), and π was 0.00583 (SD
397 0.0006). Phylogenetic analyses show that mountain treeshrews are a monophyletic group with
398 two deeply divergent lineages, each present on both mountains (Figure S2, partitions and
399 substitution models in Table S2). Outgroup relationships were consistent with the phylogenetic
400 hypothesis presented in Roberts et al. (2011). The average number of nucleotide substitutions per
401 site between the two lineages is 0.013. The BEAST dating analysis suggests that the two
402 mitochondrial lineages diverged ca. 450,000 ybp (95% Highest Posterior Density, HPD,
403 346,000–631,900 ybp, Figure S3).

404 The median joining haplotype network (Figure 3) shows that the two mountain treeshrew
405 haplogroups are present on both MT and MK. Three haplotypes are found on both mountains
406 (Table S3). Including related individuals, haplogroups 1 and 2 are found in near equal proportion
407 on MK and MT (16 and 14 individuals, respectively), while haplogroup 1 is more frequent on
408 MT (46 out of 53 individuals) (Figure 4). The AMOVA on the unrelated dataset showed
409 significant differentiation between the two mountains ($F_{ST} = 0.133$, $p = 0.00812$), with 13.3% of
410 variance accounted for by differences between mountains and 86.7% within mountains. To test
411 our prediction of significant differentiation across elevations, we then divided the population into
412 high (≥ 2000 masl) and low (< 2000 masl) elevation groups on each peak. The results showed
413 that 90.42% of the total variance is accounted for by within-group variation, and 9.58% among
414 ($F_{ST} = 0.096$, $p = 0.027$). Pairwise comparisons showed significant differences between high
415 elevation MK and low elevation MT ($F_{ST} = 0.15$, $p = 0.023$) and high elevation MK and high

416 elevation MT ($F_{ST} = 0.18$, $p = 0.013$); all other comparisons were not significant.

417 We performed Tajima's D test on an alignment including all unrelated individuals ($n =$
418 57) and separately on alignments with individuals from each haplogroup (haplogroup 1, $n = 43$;
419 haplogroup 2, $n = 14$) and each mountain (MK, $n = 25$; MT, $n = 32$) because unaccounted for
420 population structure can bias results even with high rates of migration among locations (Städler,
421 Haubold, Merino, Stephan, & Pfaffhuber, 2009). In all cases the test was not significant,
422 indicating a lack of evidence for recent population contraction, expansion, or selection.
423 Similarly, in the Bayesian skyline plot analysis, 95% HPD of the population change parameter
424 included zero; therefore, we cannot reject the hypothesis of zero demographic changes in the last
425 60,000 years.

427 *UCE loci: genetic diversity*

428 Pairwise kinship calculations revealed several groups of putatively related individuals.
429 After removing first-order relatives ($n = 22$ with kinship ≥ 0.18) from the dataset, 58 individuals
430 remained, including 33 from MT and 25 from MK. The nucleotide diversity of the filtered UCE
431 pseudo-haplotype alignment used in the MIGRATE-N analysis (1,664 concatenated UCE
432 alignments) for all 58 unrelated mountain treeshrews was 0.0017 (SE 0.000022). The nucleotide
433 diversity of the unfiltered alignment, including invariant loci and those with > 10 PIS (3,935
434 UCE alignments) was 0.0015 (SE 0.000016). Using the SNP dataset with no missing data,
435 average individual heterozygosity for all 80 individuals was 0.23 (SD 0.027), and the average
436 inbreeding coefficient (F_{IS}) was 0.012 (SD 0.12). For the 58 unrelated individuals, average
437 heterozygosity was 0.23 (SD 0.027), and F_{IS} was 0.019 (SD 0.12). Bartlett's test revealed that
438 the variances in observed and expected heterozygosity were not significantly different ($K^2 =$
439 1.68, $p = 0.2$). Average F_{IS} was higher on MK than MT, but the difference was not significant
440 (0.04 and 0.01 respectively, Welch two-sample t-test $p = 0.2$). Using the dataset with 10%
441 missing data, the probability of two individuals having identical genotypes assuming siblings are
442 present (P_{IDSib}) was 1.54×10^{-199} .

443

444 *Population Structure*

445 Both DAPC and STRUCTURE indicated that the most likely number of population

446 clusters was two and the second most likely was three, as determined by BIC and the ΔK
447 method, respectively. The ΔK method is biased toward $K = 2$ (Janes et al., 2017; Campana, Hunt,
448 Jones, & White, 2011) and simulation studies have shown that the mean probability
449 (MeanLnP(K)) output from STRUCTURE performs better in scenarios with high gene flow and
450 low F_{ST} (Latch, Dharmarajan, Glaubitz, & Rhodes, 2006). Because $K = 3$ produced the highest
451 MeanLnP(K) in STRUCTURE (Table S4a), we consider this a relevant model and show the
452 proportion of individual membership in each cluster as defined by each of the two analyses for
453 both $K = 2$ and $K = 3$ (Figure 5). Results with higher K values are shown in Figure S4. We also
454 ran STRUCTURE separately for individuals caught on MK and MT, with settings described
455 above except we ran simulations for $K = 1-5$. We found no evidence of structure among MK
456 individuals; MT individuals were divided into two clusters - one with individuals ≥ 2000 masl
457 and one with individuals < 2000 masl, with individuals of mixed ancestry at 2000 masl (Tables
458 S4b & S4c).

459 Cluster membership is mostly concordant between DAPC and STRUCTURE, except
460 STRUCTURE assigned mixed ancestry to many individuals while DAPC did not. This is not
461 unexpected as previous studies have shown that DAPC may underestimate admixture (Frosch et
462 al., 2014) while STRUCTURE is more accurate at assigning mixed ancestry (Bohling, Adams &
463 Waits, 2012). When $K = 2$, individuals at 2000 and 2400 masl on MT form a separate cluster
464 from low elevation MT + MK (Figures 4 & 5), with mixed ancestry individuals at 2000 masl
465 MT. This shows that the most prominent population subdivision does not separate the two
466 mountains or high and low elevations on MK as we predicted; rather, high elevation MT is
467 distinct. For $K = 3$, the divisions are between high elevation MT, low elevation MT, and MK,
468 with individuals at Poring Hot Spring on the eastern slope of MK (900 masl) and 2000 masl MT
469 assigned mixed ancestry (Figure 5). This suggests that no significant substructure exists among
470 MK individuals despite the greater elevational range on this mountain, and that gene flow occurs
471 between MK and MT.

472 The PCA shows a similar pattern. PC1 (7% variation explained) separates the two
473 mountains, with overlap among individuals at 900 masl. PC2 (4% variation explained) partially
474 separates individuals by elevation, with lower elevation individuals at the midline and right of
475 center, and high elevation individuals on the left (Figure 6). The “horseshoe” shape of the plot is

476 typical in isolation-by-distance (IBD) scenarios where genetic similarity decays with
477 geographical distance (Novembre & Stephens, 2008). Because of the spatial pattern evident in
478 our PCA, we ran a spatial PCA analysis (sPCA, Jombart, 2008), which explicitly incorporates
479 spatial autocorrelation between samples and allows for the visualization of genetic structure in
480 space. The results showed the greatest differentiation between high elevation MT and MK, with
481 weaker, intermediate differentiation separating individuals at low elevation MT and Poring Hot
482 Springs (Figure S5).

483 With $K = 2$, after removing individuals that could not be assigned to a STRUCTURE
484 cluster (cutoff q_k value < 0.6), F_{ST} is 0.05 ($p = 0.0001$). The AMOVA showed that most variation
485 (95%) is partitioned within clusters and only 5% between them. With $K = 3$, removing
486 individuals with q_k values < 0.6 , F_{ST} between MK and low elevation MT was 0.035 ($p = 0.001$),
487 between MK and high elevation MT 0.092 ($p = 0.0001$), and between low elevation MT and high
488 elevation MT $F_{ST} = 0.065$ ($p = 0.0005$) (Tables 2a & 2b). The AMOVA showed that 94% of
489 variation is distributed within clusters, and 6% among them.

490 Including data for all 80 individuals, the Mantel test revealed a significant, positive
491 correlation between genotypic distance and geographic distance ($r = 0.287$, $p = 0.0001$).
492 Including only the 58 unrelated individuals, the correlation was weaker but statistically
493 significant ($r = 0.05$, $p < 0.0001$). The correlogram showed significant positive autocorrelation
494 between individuals at distances of 200 m and less ($r = 0.091$, p r -rand $\geq p$ r -data = 0.0001) and
495 between 200 m and 1 km ($r = 0.036$, p r -rand $\geq p$ r -data = 0.0001); autocorrelation was no longer
496 significant at 2 km ($r = -0.001$, p r -rand $\geq p$ r -data = 0.598). At subsequent distance classes (5,
497 10, 15, and 18 km), individuals have greater genetic distance than expected at random (p r -rand
498 $\leq p$ r -data = 0.009, 0.0001, 0.0001, 0.0001, respectively) (Figure S6). The average geographic
499 distance between pairs of first-order relatives (e.g. parent-offspring or sibling pairs) was 162.5
500 m, second order (e.g. half siblings or grandparents-grand-offspring pairs) was 1.2 km, third order
501 was 4.8 km, and between distant or 'unrelated' individuals was 12 km (Table 1); this suggests
502 that in a single generation, individuals on average are unlikely to disperse beyond 162.5 m.
503 Differences between first and third, first and distant, second and distant, and third and distant
504 relatives were significant ($p < 0.05$).

505

506 *Population and migration models*

507 Model 4 (Figure 2) was the best fit model as determined by Bayes Factors in the
508 MIGRATE-N analysis, followed by Model 5 (Table S5); this was consistent across both runs of
509 the program with alternative phasing. Model 4 divided the population into three groups: high
510 elevation MT, low elevation MT, and MK, with high rates of bidirectional migration between all
511 pairs (Table S6). Model 5 divides the population into high elevation MT and low elevation MT +
512 MK with bidirectional migration (Figure 2). Across models, the mean migration rate from high
513 elevation MT to MK was greater than from MK to MT (1.3–19×, Table S6).

514 The results from NeEstimator suggest a larger effective population size on MT (< 2000
515 masl + ≥ 2000 masl) than MK despite less available habitat on MT (250 vs. 125 breeding
516 founders, respectively; Table 2 and Supplemental Information).

517

518 **Discussion**

519

520 *Levels of gene flow across elevations*

521 Our results are not consistent with Janzen's hypothesis (Janzen, 1967), which predicts
522 narrow elevational distribution and restricted gene flow across elevational gradients in tropical
523 montane species (Ghalambor et al., 2006). We report evidence of high gene flow between MK
524 and MT as well as between low and high elevations on both peaks, indicating that neither the
525 lowland habitat connecting the two peaks, nor the steep elevational gradient across which
526 mountain treeshrews occur on each peak, has significantly limited effective dispersal.

527 The KNP mountain treeshrew population is best described as comprising two or three
528 clusters, but the primary subdivision does not correspond to the two peaks or separate high and
529 low elevation MK as predicted. Rather, the summit region of MT was consistently recovered as
530 distinct in both STRUCTURE and DAPC (Figure 5a). When dividing the population into three
531 clusters, low elevation individuals at Poring Hot Springs on the eastern slope of MK show mixed
532 ancestry with low elevation MT (Figure 5b). Additionally, the MIGRATE-N analysis supports
533 the division of individuals into three population clusters (high elevation MT, low elevation MT,
534 and MK), with high migration rates between all pairs (Figure 2, Table S6). If gene flow were
535 restricted due to limited elevational dispersal or selection against cross-elevation migrants, we

536 would expect to find greater genetic differentiation on MK because of the broader elevational
537 range and associated diversity of environmental factors on this slope compared to MT. However,
538 the summit of MT was consistently recovered as the most distinct population cluster while
539 individuals caught along the entire elevational gradient on MK form a single cluster (Figures 4 &
540 5). This suggests that elevation and covarying environmental conditions are not the primary
541 variables influencing mountain treeshrew genetic structure in KNP.

542 The first prediction of Janzen's (1967) hypothesis, that tropical montane species tend to
543 have narrower elevational ranges than those in the temperate zone, has been shown to apply
544 across taxonomic groups including endotherms like birds (Ghalambor et al., 2006) and bats
545 (McCain, 2009). However, McCain (2009) found that in rodents there was either no relationship
546 between elevational range and latitude or range size increased with decreasing latitude. This
547 finding could be explained by the presence of cryptic species pairs or genetic differentiation
548 separating low and high elevation populations. Supporting this hypothesis, some studies of small
549 mammals in Southeast Asia have found strong, cryptic genetic differentiation across elevations,
550 for example, in squirrels (den Tex, Thorington, Maldonado, & Leonard, 2010; Hinckley,
551 Hawkins, Achmadi, Maldonado, & Leonard, 2020), shrews (Eldridge, Achmadi, Giarla, Rowe,
552 & Esselstyn, 2018), and mice (Heaney et al., 2011; Justiniano et al., 2015). However, McCain
553 (2009) hypothesized that rodents may cope with the lower temperatures associated with
554 increasing altitude through behavioral adaptations. Our finding of high gene flow across a broad
555 elevational extent in mountain treeshrews is not inconsistent with McCain's hypothesis. In
556 addition, Hinckley et al. (in review) found that mountain treeshrews exhibit ecophenotypic
557 changes associated with elevation, including significantly smaller ears and tails and denser hair
558 at higher elevations; these patterns were consistent on both MT and MK. Hinckley et al. suggest
559 that these phenotypic changes, in combination with behaviors including diurnal activity patterns
560 and nesting, may allow the species to persist across broad environmental conditions which is rare
561 among small mammals in this landscape (Camacho-Sanchez et al., 2019; Hinckley et al., in
562 review; Nor, 2001). Further research is necessary to determine whether the phenotypic changes
563 observed in mountain treeshrews in KNP are due to phenotypic plasticity, adaptive
564 differentiation despite gene flow, or a combination of these factors.

565

566 *Population genetic structure shaped by IBD and historical dynamics*

567 The population genetic pattern observed is partly consistent with IBD, as evidenced by 1)
568 the small, but significant, positive correlation between pairwise geographic distance and genetic
569 distance, 2) spatial autocorrelation between samples drops off at a distance of 2 km (Figure S6),
570 and 3) pairwise F_{ST} between the non-adjacent MT summit and MK clusters is greater than the
571 value between neighboring clusters (Table 2a). High gene flow rates between adjacent demes
572 across the landscape, with relatively short dispersal distances as suggested by the correlogram
573 (Figure S6) and ANOVA (Table 1), could have generated the clinal pattern we observe (Figure
574 5); however, this does not explain the distinctiveness of the summit MT cluster. The Euclidean
575 distance between the lowest and highest sampled points on MK (ca. 13.5 km) is greater than the
576 distance between the lowest and highest sampling points on MT (ca. 4.5 km), yet there is more
577 population genetic differentiation on MT. This indicates that the structure we observe is not due
578 to isolation-by-distance or isolation-by-elevation alone, and that genetic similarity decays with
579 geographic distance at unequal rates in this landscape (Figure S7a).

580 Historical population dynamics likely contributed to the observed population genetic
581 structure. Without data from other Bornean localities, it is difficult to determine what process(es)
582 generated the pattern. However, we suggest a plausible scenario given known information about
583 the relative ages of MT and MK and the degree of divergence between the mountain treeshrew
584 and its sister species. MT reached its current elevation earlier (ca. 11–7 Mya) than MK (ca. 1
585 Mya) (Collenette, 1964; Hall, 1998; Liew, Schilthuisen, & bin Lakim, 2010). This suggests that
586 MT was available for colonization prior to the split of mountain treeshrews from ruddy
587 treeshrews ca. 4 Mya (Roberts et al., 2011). If mountain treeshrews were resident on MT prior to
588 a second colonization event, this could explain the signature of two population clusters. We find
589 higher-than-average genetic diversity among individuals at high elevation MT despite its smaller
590 habitat area (Figures 1a & S7b), which is consistent with our hypothesis that this region
591 maintained a relatively stable, or recently reduced, effective population size over time relative to
592 MK. The lower rate of gene flow upslope to high elevation MT relative to gene flow towards
593 MK that we observed in the MIGRATE-N analysis (Table S6) may have preserved the signature
594 of this cluster. It is not clear what factors may be limiting upslope gene flow, but one hypothesis
595 is that it is related to a significant shift in the plant community that occurs between 1450 masl

596 and the summit (van der Ent, Cardace, Tibbett, & Echevarria, 2018). Supporting this hypothesis,
597 trapping success of mountain treeshrews and other small mammals is low from 1500 to 1800
598 masl, and increases above 2000 masl (Camacho-Sanchez et al., 2019). In addition, Hinckley et
599 al. (in review) show differences in musculature related to mastication across elevations, and
600 suggest that these differences may be due to changes in the plant community, i.e., there are fewer
601 fruiting trees at high elevations and a larger portion of invertebrates like beetles in the mountain
602 treeshrew diet.

603 By contrast, the lack of differentiation across MK could have been influenced by an
604 upslope shift at the mountain treeshrew's upper elevational limit enabled by climate warming
605 and upslope shifts in montane forest since the Last Glacial Maximum (LGM) (Cannon, Morley,
606 & Bush, 2009; Hall et al., 2009). Upslope shifts in montane forest during this period of warming
607 could have enabled range expansion at high elevations, in addition to range contraction at low
608 elevations. Mountain treeshrews on MT likely did not experience a concurrent upslope range
609 shift since MT has a much lower summit which, unlike the summit of MK, was never covered in
610 ice (Hall et al., 2009). The lack of a population expansion signature in the mountain treeshrew
611 mitogenome data could be explained by unrestricted gene flow between adjacent areas during
612 expansion (Pierce, Gutierrez, Rice, & Pfennig, 2017). As predicted for a recent expansion, we
613 find lower-than-average genetic diversity among high elevation MK individuals (≥ 1600 masl) in
614 our SNP data using estimated effective migration surface modeling (Petkova, Novembre, &
615 Stephens, 2016) to visualize genetic diversity on the landscape (Figure S7b).

616

617 *Mito-nuclear discordance*

618 The population genetic pattern inferred from our mitogenome data is discordant with the
619 nuclear SNP dataset, although it is not inconsistent with a scenario of two colonization events to
620 KNP. Phylogenetic analyses revealed two divergent mitochondrial lineages within mountain
621 treeshrews; both lineages are found on both mountains, but haplogroups 1 and 2 are equally
622 represented on MK while haplogroup 1 is more frequent on MT (Figures 3 & 4). As mentioned
623 above, MT provided montane habitat earlier than MK. If KNP were colonized a second time by
624 mountain treeshrews from the Crocker Range, this would explain the presence of two sympatric,
625 divergent lineages within Kinabalu Park. The greater frequency of haplogroup 2 on MK could be

626 explained by the closer geographic proximity of MK to the Crocker Range (Figure S8),
627 combined with male-biased dispersal limiting the movement of haplogroup 2 from MK to MT.
628 There is no information on dispersal differences between sexes in mountain treeshrews. Male-
629 biased dispersal is common among mammals (Greenwood, 1980), but female-biased dispersal
630 has been documented in the large treeshrew (Munshi-South, 2008). Lack of recombination in the
631 mitochondrial genome would have retained the signature of divergence between the two
632 haplogroups whereas recombination in nuclear SNPs would result in genetic admixture between
633 the two groups.

634 This pattern could also be the result of a single colonization event of two sympatric
635 lineages that diverged elsewhere in Borneo, for example, due to isolation in interglacial refugia
636 and mixing during glacial maxima when montane forest was at its maximum extent (Cannon et
637 al., 2009; den Tex et al, 2010). However, this scenario implies that the colonization of KNP by
638 mountain treeshrews would have occurred after the divergence between the two lineages ca.
639 450,000 ybp, which is relatively recent compared to the age of MT (at least 7 million years) and
640 the age of the species (ca. 4 million years). Additionally, multiple colonization events to MK
641 have been inferred in other taxa, including plants in the genus *Rhododendron* (Merckx et al.,
642 2015).

643 Gawin et al. (2014) documented a similar pattern in mountain blackeyes (*Chlorocharis*
644 *emiliae*) in Borneo; they found two divergent mitochondrial haplogroups on MK, with one
645 lineage sister to a lineage found on Mt. Trus Madi, a mountain south of MK within the Crocker
646 Range (Figure S8). The pattern inferred from SNP data in a subsequent study was not
647 concordant, with a single lineage found on MK (Manthey et al., 2017). This similar pattern may
648 indicate a common colonization history between mountain blackeyes and mountain treeshrews.
649 Future studies should include broader geographic sampling of mountain treeshrews, including
650 individuals from across the Crocker Range, to test the hypothesis of multiple colonization events
651 and to determine the phylogeographic history of this species in Borneo.

652
653 *UCEs for fine-scale population genomics*

654 Here, we show that sequence capture of ca. 5,000 UCEs yielded two highly informative
655 datasets (i.e. SNPs and phased pseudo-haplotype sequences) suitable for population genomics on

656 a fine spatial scale. These datasets resolved patterns of fine-scale, weak population structure in
657 mountain treeshrews within KNP, an area of approximately 754 km². The SNP dataset provided
658 sufficient statistical power to identify individuals with high probability ($P_{ID_{sib}} = 1.54 \times 10^{-199}$), to
659 identify putative family groups using pairwise kinship estimates, and to reveal patterns of
660 population structure with low levels of differentiation (Figures 5a & 5b, Tables 2a & 2b).

661 Although our results suggest that UCE loci may be sufficiently variable for population
662 genomic studies, more research is necessary to determine the substitution rate of these markers
663 and its effect on demographic parameters derived from the site-frequency spectrum (Winker et
664 al, 2018). Previous studies have suggested that the highly conserved cores of UCE loci are
665 subject to strong purifying selection. While the strength of selection decreases and the
666 substitution rate increases with distance from the core (Katzman et al. 2007), UCE-flanking
667 regions may have lower diversity than other genomic markers, leading to an excess of rare alleles
668 (Cvijović, Good, & Desai, 2018).

669 UCEs are valuable for studying species like the mountain treeshrew for which few
670 genomic resources are available. RAD-seq methods also do not require reference genomes and
671 can generate an order of magnitude more loci than UCE-based methods; this dense genomic
672 sampling enables investigation of both neutral and adaptive differentiation (Hohenlohe et al.,
673 2010), which is particularly important for defining conservation units (Funk, McKay,
674 Hohenlohe, & Allendorf, 2012). However, for inferences regarding population structure and
675 gene flow, it has been shown that fewer than 100 informative SNP loci are sufficient (von
676 Thaden et al., 2020) and here we analyzed 1,794 independent SNPs. Additionally, the average
677 heterozygosity of our UCE-derived SNPs is 0.23, similar to that reported in RAD-seq studies of
678 other small mammal populations, including mice of the genera *Apodemus* (0.28, Cerezo, Kucka,
679 Zub, Chan, & Bryk, 2020) and *Peromyscus* (0.148-0.239, Garcia-Elfring, Barrett, & Millien,
680 2019).

681 In summary, although more research is needed into the substitution rate of UCE loci and
682 its effect on demographic inferences, our results show that UCE capture methods can be used for
683 fine-scale population genomics, providing an additional tool for studying non-genome enabled
684 species. UCE capture produces data with similar information content and has several benefits
685 over RAD-seq, including 1) enabling the direct comparison of inferences drawn from the same

686 set of loci across species, allowing conclusions to be drawn about the effects of historical
687 processes on diverse taxa (Lim et al., 2020), 2) offering repeatability such that studies can
688 compare inferences for the same species across time and geographic regions (Harvey et al.,
689 2016), and 3) enabling the use of low-quality DNA, including DNA derived from historical
690 museum specimens (Hawkins et al., 2016; Lim et al., 2020; Lim & Braun, 2016, Tsai et al.,
691 2019).

692

693 *Conservation Implications*

694 As a tropical montane species, the mountain treeshrew may be impacted by global
695 climate change, which is predicted to shift montane communities in KNP upslope ca. 490 m by
696 2100 CE (Camacho-Sanchez et al., 2018; Still, 1999) assuming mild Intergovernmental Panel on
697 Climate Change scenarios (IPCC 2013, www.ipcc.ch/report/ar5/wg1/). Although the factors that
698 limit the mountain treeshrew at its lower elevational boundary are unknown, assuming that the
699 species tracks the predicted 490 m upslope shift - whether because of climatic limitations or
700 ecological interactions with lowland species expanding upslope - we predict that it will
701 experience range contraction. The species already occupies the upper elevational limits within
702 KNP, so an upslope shift in the lower bound of its distribution could not be countered with
703 expansion at its upper limit. The lack of strong population structure across elevations means that
704 upslope dispersal of lower elevation mountain treeshrews on MK will likely not increase
705 extinction risk by introducing maladaptive genetic diversity (Weiss-Lehman & Shaw, 2019).
706 However, reduction in available habitat could make the species vulnerable.

707 We also predict that in this scenario of upslope habitat shifts, mountain treeshrews would
708 maintain connectivity between MK and MT. However, the Crocker Range has few peaks above
709 1400 masl, and connectivity between KNP and the rest of the Crocker Range could be severed
710 (Figure S8). This highlights the importance of KNP as a future refugium for montane species, as
711 it contains the highest peak in the region and the greatest high-elevation forested area.
712 Conservation efforts should focus on protecting forest habitat at 900 masl outside the park to
713 facilitate gene flow and preserve genetic diversity.

714

715 **Acknowledgements**

716 L. Olson, C. Thompson, and UMMZ provided *Tupaia splendidula* DNA extracts. S. Lindley and
717 the FDA donated a MiSeq sequencing kit. T. Giarla gracefully shared his SNP calling scripts. S.
718 Castañeda Rico, M-E. Ochirbat, M. Venkatraman, N. R. McInerney, A. M. Kearns, and A. W.
719 Kaganer provided helpful comments on the manuscript. K. Helgen and R. Fleischer provided
720 logistical support. Chien Lee provided the mountain treeshrew photograph. This work was
721 funded by the Spanish Government (CGL2010-21524, CGL2017-86068-P), the Smithsonian
722 Institution (*Building the Framework of Biodiversity Science: Next Generation Phylogenomics*
723 Smithsonian Grand Challenges Awards 2012 - 2014), the National Science Foundation
724 (1547168, 1717498), and the Department of Biology at George Mason University. Logistical
725 support was provided by Laboratorio de Sistemas de Información Geográfica y Teledetección de
726 la Estación Biológica de Doñana and Doñana ICTS-RBD. We also wish to thank three
727 anonymous reviewers for comments that greatly improved the quality of this manuscript.

728

729 **Data Accessibility**

730 -DNA sequences: GenBank accessions MT423905–MT423940 and MT442045–MT442052;
731 NCBI SRA PRJNA629376
732 -MIGRATE-N input file on FigShare, doi 10.25573/data.12168225

733

734

735 **Author Contributions**

736 MTRH, MCS, and JAL organized field work; MTRH and MCS conducted field work; MTRH,
737 JAL, JEM, and LDP designed the study; JAL, JEM, and LLR provided resources for the study;
738 MTRH and LDP did laboratory work; LDP wrote the manuscript and performed UCE analyses;
739 MTRH performed phylogenetic analyses; MCS contributed figures; TRW, HCL, and MGC
740 assisted in bioinformatics; MGC and JAW developed vcf2aln; all authors participated in
741 revisions and acceptance of the final version of the manuscript.

742

743 **References**

744

- 745 Andermann, T., Fernandes, A. M., Olsson, U., Töpel, M., Pfeil, B., Oxelman, B., Aleixo, A.,
746 Faircloth, B. C., & Antonelli, A. (2018). Allele phasing greatly improves the
747 phylogenetic utility of ultraconserved elements. *Systematic Biology*, 68(1), 32–46.
748 <https://doi.org/10.1093/sysbio/syy039>
- 749 Beerli, P., & Palczewski, M. (2010). Unified framework to evaluate panmixia and migration
750 direction among multiple sampling locations. *Genetics*, 185(1), 313–326.
751 <https://doi.org/10.1534/genetics.109.112532>
- 752 Beerli, P. (2005). Comparison of Bayesian and maximum-likelihood inference of population
753 genetic parameters. *Bioinformatics*, 22(3), 341–45.
754 <https://doi.org/10.1093/bioinformatics/bti803>
- 755 Bertrand, J. A. M., Bourgeois, Y. X. C., Delahaie, B., Duval, T., García-Jiménez, R., Cornuault,
756 J., Heeb, P., Milá, B., Pujol, B., & Thébaud, C. (2014). Extremely reduced dispersal and
757 gene flow in an island bird. *Heredity*, 112(2), 190–196.
758 <https://doi.org/10.1038/hdy.2013.91>
- 759 Bohling, J. H., Adams, J. R., & Waits, L. P. (2013). Evaluating the ability of Bayesian clustering
760 methods to detect hybridization and introgression using an empirical red wolf data set.
761 *Molecular Ecology*, 22(1), 74–86. <https://doi.org/10.1111/mec.12109>
- 762 Bolger, A. M., Lohse, M., & Usadel, B. (2014). Trimmomatic: A flexible trimmer for Illumina
763 sequence data. *Bioinformatics*, 30(15), 2114–2120.
764 <https://doi.org/10.1093/bioinformatics/btu170>
- 765 Bouckaert, R., Heled, J., Kühnert, D., Vaughan, T., Wu, C., Xie, D., ..., Drummond, A. J.
766 (2014). BEAST 2: A software platform for Bayesian evolutionary analysis. *PLoS*
767 *Computational Biology*, 10(4), e1003537. <https://doi.org/10.1371/journal.pcbi.1003537>
- 768 Branch, C. L., Jahner, J. P., Kozlovsky, D. Y., Parchman, T. L. & Pravosudov, V. V. (2017).
769 Absence of population structure across elevational gradients despite large phenotypic
770 variation in mountain chickadees (*Poecile gambeli*). *Royal Society Open Science*, 4(3),
771 170057. <https://doi.org/10.1098/rsos.170057>
- 772 Camacho-Sanchez, M., Quintanilla, I., Hawkins, M. T. R., Tuh Yit Yu, F., Wells, K.,
773 Maldonado, J. E. & Leonard, J. A. (2018). Interglacial refugia on tropical mountains:

774 Novel insights from the summit rat (*Rattus baluensis*), a Borneo mountain endemic.
775 *Diversity and Distributions*, 24,1252-1266. <https://doi.org/10.1111/ddi.12761>

776 Camacho-Sanchez, M., & Hawkins, M. T. R., Tuh Yit Yu, F., Maldonado, J. E., & Leonard, J.
777 A. (2019). Endemism and diversity of small mammals along two neighboring Bornean
778 mountains. *PeerJ*, 7,e7858. <https://doi.org/10.7717/peerj.7858>

779 Campana, M. G., Hunt, H. V., Jones, H., & White, J. (2011). CorrSieve: Software for
780 summarizing and evaluating Structure output. *Molecular Ecology Resources*, 11(2), 349–
781 52. <https://doi.org/10.1111/j.1755-0998.2010.02917.x>

782 Cannon, C. H., Morley, R. J., & Bush, A. B. G. (2009). The current refugial rainforests of
783 Sundaland are unrepresentative of their biogeographic past and highly vulnerable to
784 disturbance. *Proceedings of the National Academy of Sciences*, 106(27), 11188–11193.
785 <https://doi.org/10.1073/pnas.0809865106>

786 Castillo Vardaro, J. A., Epps, C. W., Frable, B. W., & Ray, C. (2018). Identification of a contact
787 zone and hybridization for two subspecies of the American pika (*Ochotona princeps*)
788 within a single protected area. *PLOS ONE*, 13(7), e0199032.
789 <https://doi.org/10.1371/journal.pone.0199032>

790 Castresana, J. (2000). Selection of conserved blocks from multiple alignments for their use in
791 phylogenetic analysis. *Molecular Biology and Evolution*, 17(4), 540–552.

792 Cerezo, M. L.M., Kucka, M., Zub, K., Chan, Y. F., & Bryk, J. (2020). Population structure of
793 *Apodemus flavicollis* and comparison to *Apodemus sylvaticus* in northern Poland based
794 on RAD-seq. *BMC Genomics*, 21(1), 241. <https://doi.org/10.1186/s12864-020-6603-3>

795 Chen, B., Cole, J. W., & Grond-Ginsbach, C. (2017). Departure from Hardy Weinberg
796 Equilibrium and Genotyping Error. *Frontiers in Genetics*, 8, 167–167.
797 <https://doi.org/10.3389/fgene.2017.00167>

798 Cheviron, Z. A., & Brumfield, R. T. (2009). Migration-selection balance and local adaptation of
799 mitochondrial haplotypes in rufous-collared sparrows (*Zonotrichia capensis*) along an
800 elevational gradient. *Evolution*, 63(6), 1593–1605. [https://doi.org/10.1111/j.1558-](https://doi.org/10.1111/j.1558-5646.2009.00644.x)
801 [5646.2009.00644.x](https://doi.org/10.1111/j.1558-5646.2009.00644.x)

- 802 Chin, L., Moran, J. A., & Clarke, C. (2010). Trap geometry in three giant montane pitcher plant
803 species from Borneo is a function of tree shrew body size. *New Phytologist*, 186(2), 461–
804 470. <https://doi.org/10.1111/j.1469-8137.2009.03166.x>
- 805 Clarke, C. M., Bauer, U., Lee, C. C., Tuen, A. A., Rembold, K., & Moran, J. A. (2009). Tree
806 shrew lavatories: A novel nitrogen sequestration strategy in a tropical pitcher plant.
807 *Biology Letters*, 5(5), 632–635. <https://doi.org/10.1098/rsbl.2009.0311>
- 808 Collenette, P. (1964). A short account of the geology and geological history of Mt. Kinabalu.
809 *Proceedings of the Royal Society of London Series B, Biological Sciences*, 161, 56-63.
- 810 Combs, M., Puckett, E. E., Richardson, J., Mims, D., & Munshi-South, J. (2017). Spatial
811 population genomics of the brown rat (*Rattus norvegicus*) in New York City. *Molecular*
812 *Ecology*, 27(1), 83–98. <https://doi.org/10.1111/mec.14437>
- 813 Conomos, M. P., Reiner, A. P., Weir, B. S., & Thornton, T. A. (2016). Model-free estimation of
814 recent genetic relatedness. *The American Journal of Human Genetics*, 98(1), 127–48.
815 <https://doi.org/10.1016/j.ajhg.2015.11.022>
- 816 Cvijović, I., Good, B. H., & Desai, M. M. (2018). The effect of strong purifying selection on
817 genetic diversity. *Genetics*, 209(4), 1235. <https://doi.org/10.1534/genetics.118.301058>
- 818 Danecek, P., Auton, A., Abecasis, G., Albers, C. A., Banks, E., DePristo, M. A., ... 1000
819 Genomes Project Analysis Group. (2011). The variant call format and VCFtools.
820 *Bioinformatics*, 27(15), 2156–58. <https://doi.org/10.1093/bioinformatics/btr330>
- 821 den Tex, R. J., Thorington, R., Maldonado, J. E., & Leonard, J. A. (2010). Speciation dynamics
822 in the SE Asian tropics: putting a time perspective on the phylogeny and biogeography of
823 Sundaland tree squirrels, *Sundasciurus*. *Molecular Phylogenetics and Evolution*, 55(2),
824 711-720. doi: 10.1016/j.ympev.2009.12.023
- 825 Do, C., Waples, R. S., Peel, D., Macbeth, G. M., Tillett, B. J., & Ovenden, J. R. (2014).
826 NeEstimator v2: Re-implementation of software for the estimation of contemporary
827 effective population size (Ne) from genetic data. *Molecular Ecology Resources*, 14(1),
828 209–14. <https://doi.org/10.1111/1755-0998.12157>
- 829 Dray, S., & Dufour, A. B. (2007). The Ade4 package: Implementing the duality diagram for
830 ecologists. *Journal of Statistical Software*, 1(4), 1-20.
831 <https://doi.org/10.18637/jss.v022.i04>

- 832 Drummond, A. J., & Rambaut, A. (2007). BEAST: Bayesian Evolutionary Analysis by Sampling
833 Trees. *BMC Evolutionary Biology*, 7(1), 214. <https://doi.org/10.1186/1471-2148-7-214>
- 834 DuBay, S. G., & Witt, C. C. (2014). Differential high-altitude adaptation and restricted gene flow
835 across a mid-elevation hybrid zone in Andean tit-tyrant flycatchers. *Molecular Ecology*,
836 23(14), 3551–3565. <https://doi.org/10.1111/mec.12836>
- 837 Earl, D. A., & vonHoldt, B. M. (2012). STRUCTURE HARVESTER: A website and program
838 for visualizing STRUCTURE output and implementing the Evanno method.
839 *Conservation Genetics Resources*, 4(2), 359–361. [https://doi.org/10.1007/s12686-011-](https://doi.org/10.1007/s12686-011-9548-7)
840 [9548-7](https://doi.org/10.1007/s12686-011-9548-7)
- 841 Eldridge, R. A., Achmadi, A. S., Giarla, T. C., Rowe, K. C., & Esselstyn, J. A. (2018).
842 Geographic isolation and elevational gradients promote diversification in an endemic
843 shrew on Sulawesi. *Molecular Phylogenetics and Evolution*, 118, 306–317.
844 <https://doi.org/10.1016/j.ympev.2017.09.018>
- 845 Emmons, L. H. (2000). *Tupai: A field study of Bornean treeshrews*. Berkeley, CA: University of
846 California Press.
- 847 Evanno, G., Regnaut, S., & Goutdet, J. (2005). Detecting the number of clusters of individuals
848 using the software STRUCTURE: A simulation study. *Molecular Ecology*, 14(8), 2611–
849 2620. <https://doi.org/10.1111/j.1365-294X.2005.02553.x>
- 850 Excoffier, L., & Lischer, H. E. L. (2010). Arlequin suite ver. 3.5: A new series of programs to
851 perform population genetics analyses under Linux and Windows. *Molecular Ecology*
852 *Resources*, 10(3), 564–567. <https://doi.org/10.1111/j.1755-0998.2010.02847.x>
- 853 Falush, D., Stephens, M., & Pritchard, J. K. (2003). Inference of population structure using
854 multilocus genotype data: Linked loci and correlated allele frequencies. *Genetics*, 164(4),
855 1567–1587.
- 856 Faircloth, B. C. (2016). PHYLUCE is a software package for the analysis of conserved genomic
857 loci. *Bioinformatics*, 32(5), 786–88. <https://doi.org/10.1093/bioinformatics/btv646>
- 858 Faircloth, B. C., McCormack, J. E., Crawford, N. G., Harvey, M. G., Brumfield, R. T., & Glenn,
859 T. C. (2012). Ultraconserved elements anchor thousands of genetic markers spanning
860 multiple evolutionary timescales. *Systematic Biology*, 61(5), 717–726.
861 <https://doi.org/10.1093/sysbio/sys004>

- 862 Feeley, K. J., Stroud, J. T., & Perez, T. M. (2017). Most ‘global’ reviews of species’ responses to
863 climate change are not truly global. *Diversity and Distributions*, 23(3), 231–234.
864 <https://doi.org/10.1111/ddi.12517>
- 865 Feijó, A., Wen, Z., Cheng, J., Ge, D., Xia, L., & Yang, Q. (2019). Divergent selection along
866 elevational gradients promotes genetic and phenotypic disparities among small mammal
867 populations. *Ecology and Evolution*, 9(12), 7080–7095.
868 <https://doi.org/10.1002/ece3.5273>
- 869 Felsenstein, J. (2005). Accuracy of coalescent likelihood estimates: Do we need more sites, more
870 sequences, or more loci? *Molecular Biology and Evolution*, 23(3), 691–700.
871 <https://doi.org/10.1093/molbev/msj079>
- 872 Frosch, C., Kraus, R. H. S., Angst, C., Allgöwer, R., Michaux, J., Teubner, J., & Nowak, C.
873 (2014). The genetic legacy of multiple beaver reintroductions in central Europe. *PLOS*
874 *ONE*, 9(5), e97619. <https://doi.org/10.1371/journal.pone.0097619>
- 875 Funk, W. C., McKay, J. K., Hohenlohe, P. A., & Allendorf, F. W. (2012). Harnessing genomics
876 for delineating conservation units. *Trends in Ecology & Evolution*, 27(9), 489–496.
877 <https://doi.org/10.1016/j.tree.2012.05.012>
- 878 Gadek, C. R., Newsome, S. D., Beckman, E. J., Chavez, A. N., Galen, S. C., Bautista, E., & Witt,
879 C. C. (2018). Why are tropical mountain passes ‘low’ for some species? Genetic and
880 stable-isotope tests for differentiation, migration and expansion in elevational generalist
881 songbirds. *Journal of Animal Ecology*, 87(3), 741–753. [https://doi.org/10.1111/1365-](https://doi.org/10.1111/1365-2656.12779)
882 [2656.12779](https://doi.org/10.1111/1365-2656.12779)
- 883 Garcia-Elfring, A., Barrett, R. D. H., & Millien, V. (2019). Genomic signatures of selection
884 along a climatic gradient in the northern range margin of the white-footed mouse
885 (*Peromyscus leucopus*). *Journal of Heredity*, 110(6), 684–695.
886 <https://doi.org/10.1093/jhered/esz045>
- 887 Gawin, D. F., Rahman, M. A., Ramji, M. F. S., Smith, B. T., Lim, H. C., Moyle, R. G., &
888 Sheldon, F.H. (2014). Patterns of avian diversification in Borneo: The case of the
889 endemic mountain black-eye (*Chlorocharis emiliae*). *The Auk*, 131(1), 86–99.
890 <https://doi.org/10.1642/AUK-13-190.1>

- 891 Ghalambor, C. K., Huey, R. B., Martin, P. R., Tewksbury, J. J., & Wang, G. (2006). Are
892 mountain passes higher in the tropics? Janzen's hypothesis revisited. *Integrative and*
893 *Comparative Biology*, 46(1), 5–17. <https://doi.org/10.1093/icb/icj003>
- 894 Giarla, T. C., Maher, S. P., Achmadi, A. S., Moore, M. K., Swanson, M. T., Rowe, K. C., &
895 Esselstyn, J. A. (2018). Isolation by marine barriers and climate explain areas of
896 endemism in an island rodent. *Journal of Biogeography*, 45(9), 2053–2066.
897 <https://doi.org/10.1111/jbi.13392>
- 898 Giarla, T. C., & Esselstyn, J. A. (2015). The challenges of resolving a rapid, recent radiation:
899 Empirical and simulated phylogenomics of Philippine shrews. *Systematic Biology*, 64(5),
900 727–740. <https://doi.org/10.1093/sysbio/syv029>
- 901 Gilbert, P. S., Wu, J., Simon, M. W., Sinsheimer, J. S., & Alfaro, M. E. (2018). Filtering
902 nucleotide sites by phylogenetic signal to noise ratio increases confidence in the Neoaves
903 phylogeny generated from ultraconserved elements. *Molecular Phylogenetics and*
904 *Evolution*, 126, 116–128. <https://doi.org/10.1016/j.ympev.2018.03.033>
- 905 Gill, B. A., Kondratieff, B. C., Casner, K. L., Encalada, A. C., Flecker, A. S., Gannon, D. G., ...,
906 Funk, W. C. (2016). Cryptic species diversity reveals biogeographic support for the
907 'mountain passes are higher in the tropics' hypothesis. *Proceedings of the Royal Society*
908 *B: Biological Sciences*, 283, 1832. <https://doi.org/10.1098/rspb.2016.0553>
- 909 Goldberg, C. S., & Waits, L. P. (2010). Quantification and reduction of bias from sampling
910 larvae to infer population and landscape genetic structure. *Molecular Ecology Resources*
911 10(2), 304–313. <https://doi.org/10.1111/j.1755-0998.2009.02755.x>
- 912 Greenwood, P. J. (1980). Mating systems, philopatry and dispersal in birds and mammals.
913 *Animal Behaviour*, 28(4), 1140–1162. [https://doi.org/10.1016/S0003-3472\(80\)80103-5](https://doi.org/10.1016/S0003-3472(80)80103-5)
- 914 Gueuning, M., Suchan, T., Rutschmann, S., Gattolliat, J., Jamsari, J., Kamil, A. I., ..., Alvarez,
915 N. (2017). Elevation in tropical sky islands as the common driver in structuring genes and
916 communities of freshwater organisms. *Scientific Reports*, 7(1), 16089.
917 <https://doi.org/10.1038/s41598-017-16069-y>
- 918 Hall, R. (1998). The plate tectonics of Cenozoic SE Asia and the distribution of land and sea. In
919 R. Hall & J. D. Holloway (Eds.) *Biogeography and the geological evolution of SE Asia*.
920 (pp. 99-131). Backhuys Publishers: Leiden, The Netherlands.

- 921 Hall, R., Cottam, M., Suggate, S., Tongkul, F., Sperber, C., & Batt, G. E. (2009). *The Geology of*
922 *Mount Kinabalu*. Sabah Parks: Sabah, Malaysia.
- 923 Harrison, R. G. (1989). Animal mitochondrial DNA as a genetic marker in population and
924 evolutionary biology. *Trends in Ecology & Evolution*, *4*(1), 6–11.
925 [https://doi.org/10.1016/0169-5347\(89\)90006-2](https://doi.org/10.1016/0169-5347(89)90006-2)
- 926 Harvey, M. G., Smith, B. T., Glenn, T. C., Faircloth, B. C., & Brumfield, R. T. (2016). Sequence
927 capture versus restriction site associated DNA sequencing for shallow systematics.
928 *Systematic Biology*, *65*(5), 910–924. <https://doi.org/10.1093/sysbio/syw036>
- 929 Hawkins, M. T. R., Leonard, J. A., Helgen, K. M., McDonough, M. M., Rockwood, L. L., &
930 Maldonado, J. E. (2016). Evolutionary history of endemic Sulawesi squirrels constructed
931 from UCEs and mitogenomes sequenced from museum specimens. *BMC Evolutionary*
932 *Biology*, *16*(1). <https://doi.org/10.1186/s12862-016-0650-z>
- 933 Heaney, L. R., Balete, D. S., Rickart, E. A., Alviola, P. A., Duya, M. R. M., Duya, M. V., ... &
934 Steppan, S. J. (2011). Seven new species and a new subgenus of forest mice (Rodentia:
935 Muridae: Apomys) from Luzon Island. *Fieldiana Life and Earth Sciences*, *2011*(2), 1-60.
- 936 Hinckley, A., Sanchez-Donoso, I., Comas, M., Camacho-Sanchez, M., Hasan, N. H., & Leonard,
937 J. A. (in review). Challenging ecogeographical rules: phenotypic variation in the
938 mountain treeshrew (*Tupaia montana*) along tropical elevational gradients.
- 939 Hinckley, A., Hawkins, M. T. R., Achmadi, A. S., Maldonado, J. E., & Leonard, J. A. (2020).
940 Ancient Divergence Driven by Geographic Isolation and Ecological Adaptation in Forest
941 Dependent Sundaland Tree Squirrels. *Frontiers in Ecology and Evolution*, *8*, 208.
942 <https://doi.org/10.3389/fevo.2020.00208>
- 943 Hohenlohe, P. A., Bassham, S., Etter, P. D., Stiffler, N., Johnson, E. A., & Cresko, W. A. (2010).
944 Population genomics of parallel adaptation in threespine stickleback using sequenced
945 RAD tags. *PLoS Genetics*, *6*(2), e1000862. <https://doi.org/10.1371/journal.pgen.1000862>
- 946 Jakobsson, M., & Rosenberg, N. A. (2007). CLUMPP: A cluster matching and permutation
947 program for dealing with label switching and multimodality in analysis of population
948 structure. *Bioinformatics*, *23*(14), 1801–1806.
949 <https://doi.org/10.1093/bioinformatics/btm233>

- 950 Janes, J. K., Miller, J. M., Dupuis, J. R., Malenfant, R. M., Gorrell, J. C., Cullingham, C. I., &
951 Andrew, R. L. (2017). The $K = 2$ conundrum. *Molecular Ecology*, 26(14), 3594–3602.
952 <https://doi.org/10.1111/mec.14187>
- 953 Janzen, D. H. (1967). Why mountain passes are higher in the tropics. *The American Naturalist*,
954 101(919): 233–249. <https://doi.org/10.1086/282487>
- 955 Jombart, T. (2008). ADEGENET: An R package for the multivariate analysis of genetic markers.
956 *Bioinformatics*, 24(11), 1403–1405. <https://doi.org/10.1093/bioinformatics/btn129>
- 957 Justiniano, R., Schenk, J. J., Balete, D. S., Rickart, E. A., Esselstyn, J. A., Heaney, L. R., &
958 Steppan, S. J. (2015). Testing diversification models of endemic Philippine forest mice
959 (*Apomys*) with nuclear phylogenies across elevational gradients reveals repeated
960 colonization of isolated mountain ranges. *Journal of Biogeography*, 42(1), 51–64.
- 961 Katoh, K., Misawa, K., Kuma, K., & Miyata, T. (2002). MAFFT: A novel method for rapid
962 multiple sequence alignment based on fast fourier transform. *Nucleic Acids Research*,
963 30(14), 3059–3066. <https://doi.org/10.1093/nar/gkf436>
- 964 Katzman, S., Kern, A. D., Bejerano, G., Fewell, G., Fulton, L., Wilson, R. K., Salama, S. R., &
965 Haussler, D. (2007). Human genome ultraconserved elements are ultraselected. *Science*,
966 317(5840), 915. <https://doi.org/10.1126/science.1142430>
- 967 Khaliq, I., Hof, C., Prinzing, R., Böhning-Gaese, K., & Pfenninger, M. (2014). Global
968 variation in thermal tolerances and vulnerability of endotherms to climate change.
969 *Proceedings of the Royal Society Biological Sciences*, 281, 20141097.
970 <https://doi.org/10.1098/rspb.2014.1097>
- 971 Kitayama, K. (1992). An altitudinal transect study of the vegetation on Mount Kinabalu, Borneo
972 *Vegetatio*, 102(2), 149–171. www.jstor.org/stable/20046210
- 973 Kumar, S., Stecher, G., & Tamura, K. (2016). MEGA7: Molecular evolutionary genetics analysis
974 version 7.0 for bigger datasets. *Molecular Biology and Evolution*, 33(7), 1870–1874.
975 <https://doi.org/10.1093/molbev/msw054>
- 976 Lanfear, R., Calcott, B., Ho, S. Y. W., & Guindon, S. (2012). PartitionFinder: Combined
977 selection of partitioning schemes and substitution models for phylogenetic analyses.
978 *Molecular Biology and Evolution*, 29(6), 1695–1701.
979 <https://doi.org/10.1093/molbev/mss020>

- 980 Latch, E. K., Dharmarajan, G., Glaubitz, J. C., & Rhodes, O. E. (2006). Relative performance of
981 Bayesian clustering software for inferring population substructure and individual
982 assignment at low levels of population differentiation. *Conservation Genetics*, 7(2), 295–
983 302. <https://doi.org/10.1007/s10592-005-9098-1>
- 984 Leigh, J. W., & Bryant, D. (2015). Popart: Full-feature software for haplotype network
985 construction. *Methods in Ecology and Evolution*, 6(9), 1110–1116.
986 <https://doi.org/10.1111/2041-210X.12410>
- 987 Lenoir, J., & Svenning, J. C. (2015). Climate-related range shifts - a global multidimensional
988 synthesis and new research directions. *Ecography*, 38(1), 15–28.
989 <https://doi.org/10.1111/ecog.00967>
- 990 Li, H. (2013). Aligning sequence reads, clone sequences and assembly contigs with BWA-MEM.
991 *ArXiv* 1303.3997v1.
- 992 Li, H., Handsaker, B., Wysoker, A., Fennell, T., Ruan, J., Homer, N., ..., 1000 Genome Project
993 Data Processing Subgroup. (2009). The Sequence Alignment/Map format and SAMtools.
994 *Bioinformatics*, 25(16), 2078–2079. <https://doi.org/10.1093/bioinformatics/btp352>
- 995 Librado, P., & Rozas, J. (2009). DnaSP v5: A software for comprehensive analysis of DNA
996 polymorphism data. *Bioinformatics*, 25(11), 1451–1452.
997 <https://doi.org/10.1093/bioinformatics/btp187>
- 998 Liew, T. S., Schilthuizen, M., & bin Lakim, M. (2010). The determinants of land snail diversity
999 along a tropical elevational gradient: Insularity, geometry and niches. *Journal of*
1000 *Biogeography*, 37(6), 1071–1078. <https://doi.org/10.1111/j.1365-2699.2009.02243.x>
- 1001 Lim, H. C., and Braun, M. J. (2016). High-throughput SNP genotyping of historical and modern
1002 samples of five bird species via sequence capture of ultraconserved elements. *Molecular*
1003 *Ecology Resources*, 16(5), 1204–1223. <https://doi.org/10.1111/1755-0998.12568>
- 1004 Lim, H. C., Shakya, S. B., Harvey, M. G., Moyle, R. G., Fleischer, R. C., Braun, M. J., &
1005 Sheldon, F. H. (2020). Opening the door to greater phylogeographic inference in
1006 Southeast Asia: Comparative genomic study of five codistributed rainforest bird species
1007 using target capture and historical DNA. *Ecology and Evolution*, 10, 3222–3247.
1008 <https://doi.org/10.1002/ece3.5964>

- 1009 Linck, E., Freeman, B. G., & Dumbacher, J. P. (2019). Speciation and gene flow across an
1010 elevational gradient in New Guinea kingfishers. *BioRxiv*, 589044.
1011 <https://doi.org/10.1101/589044>
- 1012 Manichaikul, A., Mychaleckyj, J. C., Rich, S. S., Daly, K., Sale, M., & Chen, W. M. (2010).
1013 Robust relationship inference in genome-wide association studies. *Bioinformatics*,
1014 26(22), 2867–2873. <https://doi.org/10.1093/bioinformatics/btq559>
- 1015 Manthey, J. D., Moyle, R. G., Gawin, D. F., Rahman, M. A., Ramji, M. F. S., & Sheldon, F. H.
1016 (2017). Genomic phylogeography of the endemic mountain black-eye of Borneo
1017 (*Chlorocharis emiliae*): Montane and lowland populations differ in patterns of
1018 Pleistocene diversification. *Journal of Biogeography*, 44(10), 2272–2283.
1019 <https://doi.org/10.1111/jbi.13028>
- 1020 Mason, N. A., Olvera-Vital, A., Lovette, I. J., & Navarro-Sigüenza, A. G. (2018). Hidden
1021 endemism, deep polyphyly, and repeated dispersal across the Isthmus of Tehuantepec:
1022 Diversification of the white-collared seedeater complex (Thraupidae: *Sporophila*
1023 *torqueola*). *Ecology and Evolution*, 8(3): 1867–1881. <https://doi.org/10.1002/ece3.3799>
- 1024 McCain, C. M. 2009. Vertebrate range sizes indicate that mountains may be ‘higher’ in the
1025 tropics. *Ecology Letters*, 12(6), 550–560. [https://doi.org/10.1111/j.1461-](https://doi.org/10.1111/j.1461-0248.2009.01308.x)
1026 [0248.2009.01308.x](https://doi.org/10.1111/j.1461-0248.2009.01308.x)
- 1027 McKenna, A., Hanna, M., Banks, E., Sivachenko, A., Cibulskis, K., Kernytzky, A., ..., DePristo,
1028 M. A. (2010). The Genome Analysis Toolkit: A MapReduce framework for analyzing
1029 next-generation DNA sequencing data. *Genome Research*, 20(9), 1297–1303.
1030 <https://doi.org/10.1101/gr.107524.110>
- 1031 McKinney, G. J., Waples, R. K., Seeb, L. W., & Seeb, J.E. 2017. Paralogs are revealed by
1032 proportion of heterozygotes and deviations in read ratios in genotyping-by-sequencing
1033 data from natural populations. *Molecular Ecology Resources*, 17(4): 656–669.
1034 <https://doi.org/10.1111/1755-0998.12613>
- 1035 Merckx, V. S. F. T., Hendriks, K. P., Beentjes, K. K., Mennes, C. B., Becking, L. E.,
1036 Peijnenburg, K. T. C. A., ..., Schilthuizen, M. (2015). Evolution of endemism on a young
1037 tropical mountain. *Nature*, 524(7565), 347–350. <https://doi.org/10.1038/nature14949>

- 1038 Moritz, C. (1994). Defining ‘evolutionarily significant units’ for conservation. *Trends in Ecology*
1039 & *Evolution*, 9(10), 373–375. [https://doi.org/10.1016/0169-5347\(94\)90057-4](https://doi.org/10.1016/0169-5347(94)90057-4)
- 1040 Muenchow, J., Dieker, P., Kluge, J., Kessler, M., & von Wehrden, H. (2018). A review of
1041 ecological gradient research in the tropics: Identifying research gaps, future directions,
1042 and conservation priorities. *Biodiversity and Conservation*, 27(2), 273–285.
1043 <https://doi.org/10.1007/s10531-017-1465-y>
- 1044 Munshi-South, J. (2008). Female-biased dispersal and gene flow in a behaviorally monogamous
1045 mammal, the large treeshrew (*Tupaia tana*). *PLoS ONE*, 3(9), e3228.
1046 <https://doi.org/10.1371/journal.pone.0003228>
- 1047 Nor, S.M. (2001). Elevational diversity patterns of small mammals on Mount Kinabalu, Sabah,
1048 Malaysia. *Global Ecology and Biogeography*, 10(1): 41–62.
1049 <https://doi.org/10.1046/j.1466-822x.2001.00231.x>
- 1050 Novembre, J., & Stephens, M. (2008). Interpreting principal component analyses of spatial
1051 population genetic variation. *Nature Genetics*, 40(5), 646–649.
1052 <https://doi.org/10.1038/ng.139>
- 1053 Oswald, J. A., Harvey, M. G., Rensen, R. C., Foxworth, D. U., Cardiff, S. W., Dittmann, D. L.,
1054 ..., Brumfield, R. T. (2016). Willet be one species or two? A genomic view of the
1055 evolutionary history of *Tringa semipalmata*. *The Auk*, 133(4), 593–614.
1056 <https://doi.org/10.1642/AUK-15-232.1>
- 1057 Payne, J., Francis, C. M., & Phillipps, K. (2016). *A Field Guide to the Mammals of Borneo*. The
1058 Sabah Society: Kota Kinabalu, Sabah, Malaysia.
- 1059 Peakall, R., & Smouse, P. E. (2012). GenA1Ex 6.5: Genetic analysis in Excel. Population genetic
1060 software for teaching and research-an update. *Bioinformatics*, 28(19), 2537–2539.
1061 <https://doi.org/10.1093/bioinformatics/bts460>
- 1062 Petkova, D., Novembre, J., & Stephens, M. (2016). Visualizing spatial population structure with
1063 estimated effective migration surfaces. *Nature Genetics*, 48(1): 94–100.
1064 <https://doi.org/10.1038/ng.3464>
- 1065 Pierce, A. A., Gutierrez, R., Rice, A. M., & Pfennig, K.S. (2017). Genetic variation during range
1066 expansion: effects of habitat novelty and hybridization. *Proceedings of the Royal Society*
1067 *B: Biological Sciences*, 284(1852). <https://doi.org/10.1098/rspb.2017.0007>

- 1068 Polato, N. R., Gill, B. A., Shah, A. A., Gray, M. M., Casner, K. L., Barthelet, A., ..., Zamudio,
1069 K. R. (2018). Narrow thermal tolerance and low dispersal drive higher speciation in
1070 tropical mountains. *Proceedings of the National Academy of Sciences*, *115*(49), 12471–
1071 12476. <https://doi.org/10.1073/pnas.1809326115>
- 1072 Pritchard, J. K., Stephens, M., & Donnelly, P. (2000). Inference of population structure using
1073 multilocus genotype data. *Genetics*, *155*(2), 945–959.
- 1074 Roberts, T. E., Lanier, H. C., Sargis, E. J., & Olson, L. E. (2011). Molecular phylogeny of
1075 treeshrews (Mammalia: Scandentia) and the timescale of diversification in Southeast
1076 Asia. *Molecular Phylogenetics and Evolution*, *60*(3), 358–372.
1077 <https://doi.org/10.1016/j.ympev.2011.04.021>
- 1078 Ronquist, F., & Huelsenbeck, J. P. (2003). MrBayes 3: Bayesian phylogenetic inference under
1079 mixed models. *Bioinformatics*, *19*(12): 1572–1574.
1080 <https://doi.org/10.1093/bioinformatics/btg180>
- 1081 Schmitz, J., Ohme, M., & Zischler, H. (2000). The complete mitochondrial genome of *Tupaia*
1082 *belangeri* and the phylogenetic affiliation of Scandentia to other Eutherian orders.
1083 *Molecular Biology and Evolution*, *17*(9), 1334–43.
1084 <https://doi.org/10.1093/oxfordjournals.molbev.a026417>
- 1085 Smith, B. T., Harvey, M. G., Faircloth, B. C., Glenn, T. C., & Brumfield, R. T. (2014). Target
1086 capture and massively parallel sequencing of ultraconserved elements for comparative
1087 studies at shallow evolutionary time scales. *Systematic Biology*, *63*(1), 83–95.
1088 <https://doi.org/10.1093/sysbio/syt061>
- 1089 Städler, T., Haubold, B., Merino, C., Stephan, W., & Pfaffelhuber, P. (2009). The Impact of
1090 Sampling Schemes on the Site Frequency Spectrum in Nonequilibrium Subdivided
1091 Populations. *Genetics*, *182*(1), 205–216. <https://doi.org/10.1534/genetics.108.094904>
- 1092 Still, C. J., Foster, P. N., & Schneider, S. H. (1999). Simulating the effects of climate change on
1093 tropical montane cloud forests. *Nature*, *398*(6728), 608–610.
1094 <https://doi.org/10.1038/19293>
- 1095 Sturges, H. (1926). The choice of a class-interval. *Journal of the American Statistical*
1096 *Association*, *21*, 65–66.

- 1097 Tsai, W. L. E., Mota-Vargas, C., Rojas-Soto, O., Bhowmik, R., Liang, E. Y., Maley, J. M., ...,
1098 McCormack, J. E. (2019). Museum genomics reveals the speciation history of
1099 *Dendrortyx* wood-partridges in the mesoamerican highlands. *Molecular Phylogenetics*
1100 *and Evolution*, *136*, 29–34. <https://doi.org/10.1016/j.ympev.2019.03.017>
- 1101 van der Ent, A., Cardace, D., Tibbett, M., & Echevarria, G. (2018). Ecological implications of
1102 pedogenesis and geochemistry of ultramafic soils in Kinabalu Park (Malaysia). *Catena*
1103 *160*, 154–169. <https://doi.org/10.1016/j.catena.2017.08.015>
- 1104 von Thaden, A., Nowak, C., Tiesmeyer, A., Reiners, T. E., Alves, P. C., Lyons, L. A., ...
1105 Cocchiararo, B. (2020). Applying genomic data in wildlife monitoring: Development
1106 guidelines for genotyping degraded samples with reduced single nucleotide
1107 polymorphism (SNP) panels. *Molecular Ecology Resources*, *20*(3), 662–680.
1108 <https://doi.org/10.1111/1755-0998.13136>
- 1109 Waits, L. P., Luikart, G., & Taberlet, P. (2001). Estimating the probability of identity among
1110 genotypes in natural populations: Cautions and guidelines. *Molecular Ecology*, *10*(1),
1111 249–256. <https://doi.org/10.1046/j.1365-294X.2001.01185.x>
- 1112 Waples, R. S., & Do, C. (2008). Ldne: A program for estimating effective population size from
1113 data on linkage disequilibrium. *Molecular Ecology Resources*, *8*(4), 753–756.
1114 <https://doi.org/10.1111/j.1755-0998.2007.02061.x>
- 1115 Weiss-Lehman, C., & Shaw, A. K. (2019). Spatial population structure determines extinction
1116 risk in climate-induced range shifts. *The American Naturalist*, *706259*.
1117 <https://doi.org/10.1086/706259>
- 1118 Winker, K., Glenn, T. C., & Faircloth, B.C. (2018). Ultraconserved elements (UCEs) illuminate
1119 the population genomics of a recent, high-latitude avian speciation event. *PeerJ*, *6*,
1120 e5735. <https://doi.org/10.7717/peerj.5735>

1121

1122 **Table 1.** Geographical distances between pairs of individuals with different levels of estimated
1123 relatedness based on analysis with the KING software. ANOVA and Tukey Honest Significant
1124 Differences test showed significant differences in distances between all pairs except first and
1125 second-order relatives and second and third-order relatives ($p < 0.05$).

1126

Kinship	Relatedness	n	Average distance (m)	Median distance (m)	Max distance (m)
> 0.18	First order (Parent-offspring, siblings)	42	162.5	100.8	570.1
0.177 - 0.0884	Second order (e.g. half-siblings)	56	1247	322.8	25850
0.0883 - 0.0442	Third order (e.g. cousins)	112	4819	793.0	26490
< 0.044	Distant or unrelated	2932	12310	15960	29430

1127

1128

1129 **Table 2.** Effective population sizes and pairwise F_{ST} of population clusters with **a) $K = 3$** and **b)**
 1130 $K = 2$. MK, Mount Kinabalu; MT, Mount Tambuyukon. N_e estimates are on the diagonal with
 1131 95% CI in parenthesis; F_{ST} estimates are below the diagonal, with associated p -values above the
 1132 diagonal.

1133

1134 **a)**

$K = 3$	MK	MT < 2000masl	MT > 2000masl
MK (n=22)	125 (105–152)	0.00120	0.00010
MT < 2000 masl (n=19)	0.035	202 (157–282)	0.00050
MT > 2000 masl (n=11)	0.092	0.065	48 (40–59)

1135

1136

1137 **b)**

$K = 2$	MK + MT < 2000masl	MT > 2000masl
MK + MT < 2000 masl (n=36)	180 (160–205)	0.0001
MT > 2000 masl (n=18)	0.050	57 (52–63)

1138

1139

1140 **Figure text.**

1141
1142 **Figure 1a.** Map of mountain treeshrew distribution (inset modified from IUCN 2019, with a
1143 white star indicating the location of Kinabalu National Park, KNP), and a map of sampling
1144 locations within KNP, Sabah, Borneo. Park boundaries are demarcated by dashed lines, transects
1145 by black lines, and sampling locations by white circles, with elevations at each site labeled.
1146 Shading indicates the lower and upper portions of mountain treeshrew habitat, with 900–2000
1147 masl shown in medium gray and >2000 masl in dark grey. The total number of mountain
1148 treeshrews collected and the number of unrelated individuals included in our analyses at each
1149 trapping site are as follows (unrelated/total): MK 900, 6/6; 1600 5/6; 2200 5/5; 2700 4/4; 3200
1150 5/5; MT 900 4/4; 1300 4/6; 1600 4/4; 2000 14/22; 2400 7/14.

1151 **Figure 1b.** Image of a mountain treeshrew and a pitcher plant (*Nepenthes lowii*), KNP (Photo
1152 credit: Chien C. Lee). The two species exhibit a mutualistic relationship in which mountain
1153 treeshrews feed on the sugary secretions provided by the plant and in turn provide the plant
1154 phosphorous and nitrogen through feces (Chin, Moran, & Clarke, 2010).

1155
1156
1157
1158
1159 **Figure 2.** Population structure and migration models evaluated using MIGRATE-N, with model
1160 rank shown below each numbered model. The best model according to Bayes factors is model 4,
1161 followed by model 5. Log marginal likelihood values are listed in Table S5. MT, Mt.
1162 Tambuyukon; MK, Mt. Kinabalu; High \geq 2000 masl; Low $<$ 2000 masl.

1163
1164
1165
1166 **Figure 3.** Median joining network of 34 mitogenome sequences in the ‘unrelated’ dataset.
1167 Haplotypes are numbered H1-H36; H4 and H16 are not included because they were removed
1168 when close relatives were trimmed from the dataset. Dashed lines represent the number of base
1169 pair differences between haplotypes except in cases where the number of differences exceeds 40.
1170 Colors correspond to the two mountains (MT, orange; MK, blue). The two haplogroups are not

1171 shown to scale and are separated by 186 bp substitutions. Circle area is proportional to the
1172 number of individuals with each haplotype; the legend shows the size for 1 and 10 samples,
1173 respectively.

1174
1175
1176

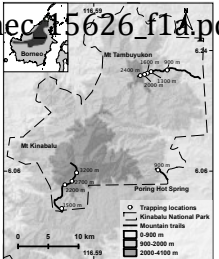
1177 **Figure 4.** Elevations sampled on Mt. Kinabalu (900, 1600, 2200, 2700, and 3200 masl) and Mt.
1178 Tambuyukon (900, 1300, 1600, 2000, and 2400 masl) with the distribution of mitochondrial
1179 haplogroups per elevation shown below each transect line and SNP clusters above. Colors of
1180 each transect line correspond to localities on inset map (dark blue, MK; light blue, Poring Hot
1181 Spring MK; orange, MT). Mitogenome pie charts indicate, for each elevation, the number of
1182 treeshrews sampled with a haplotype from mitochondrial haplogroup 1 (light grey) and 2 (dark
1183 grey). SNP pie charts indicate for each elevation the proportion of ancestry assigned to cluster 1
1184 (light grey) and cluster 2 (dark grey) by STRUCTURE with $K=2$, which was determined by the
1185 Evanno method to be the most likely number of clusters. The area of each circle is proportional
1186 the number of individuals sampled at each elevation.

1187
1188
1189

1190 **Figure 5.** Cluster membership according to DAPC and STRUCTURE for **a)** $K=2$ and **b)** $K=3$.
1191 For each analysis, $K=2$ was the best-fitting number of clusters, followed by $K=3$. Each
1192 horizontal line represents a single individual with shading showing how much of each's ancestry
1193 can be attributed to each cluster. Individuals are arranged from high elevation Mt. Tambuyukon
1194 to low elevation Mt. Tambuyukon followed by low elevation Mt. Kinabalu to high elevation Mt.
1195 Kinabalu. Elevations and mountains are labeled on the Y-axis.

1196

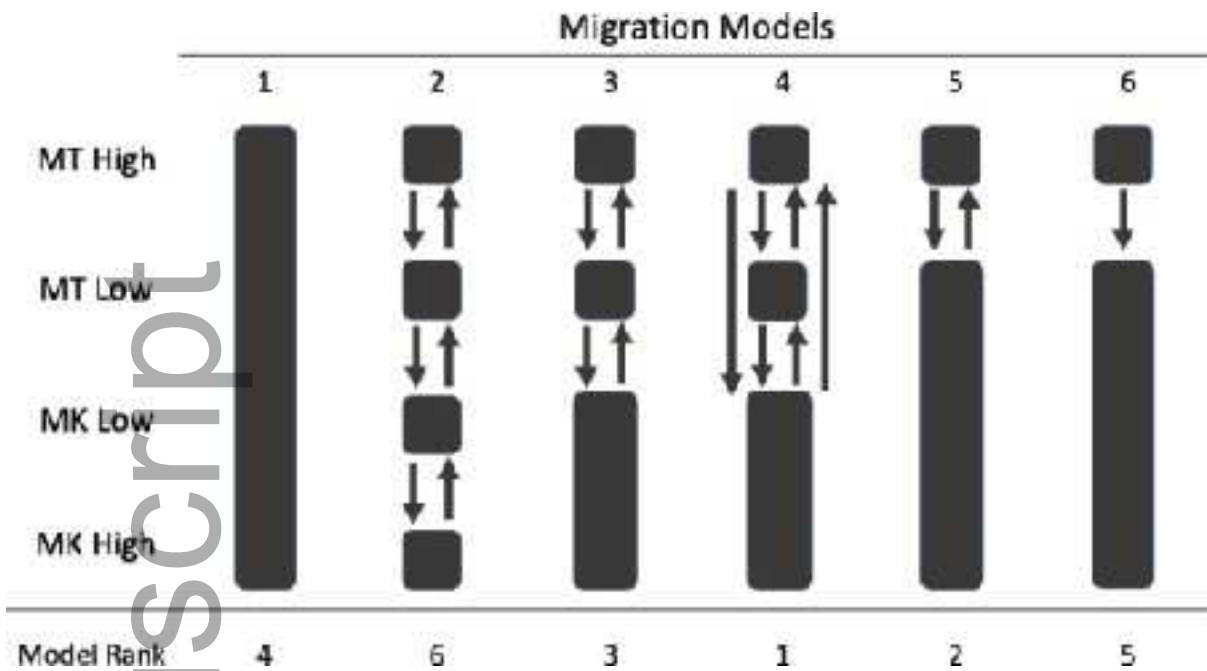
1197 **Figure 6.** PCA plot with individuals caught on Mt. Kinabalu shown in blue circles and Mt.
1198 Tambuyukon in orange triangles. Individuals sampled at lower elevations are shaded with light
1199 colors and high elevation with dark, and each point is labeled with the sampling location
1200 elevation. PC1 explains 7% of variance and PC2 explains 4%.





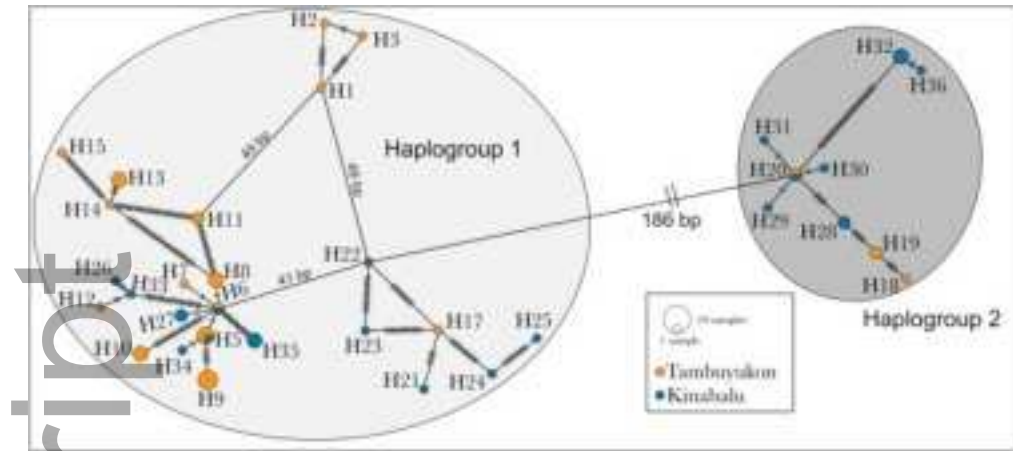
mec_15626_f1b.jpeg

Author M



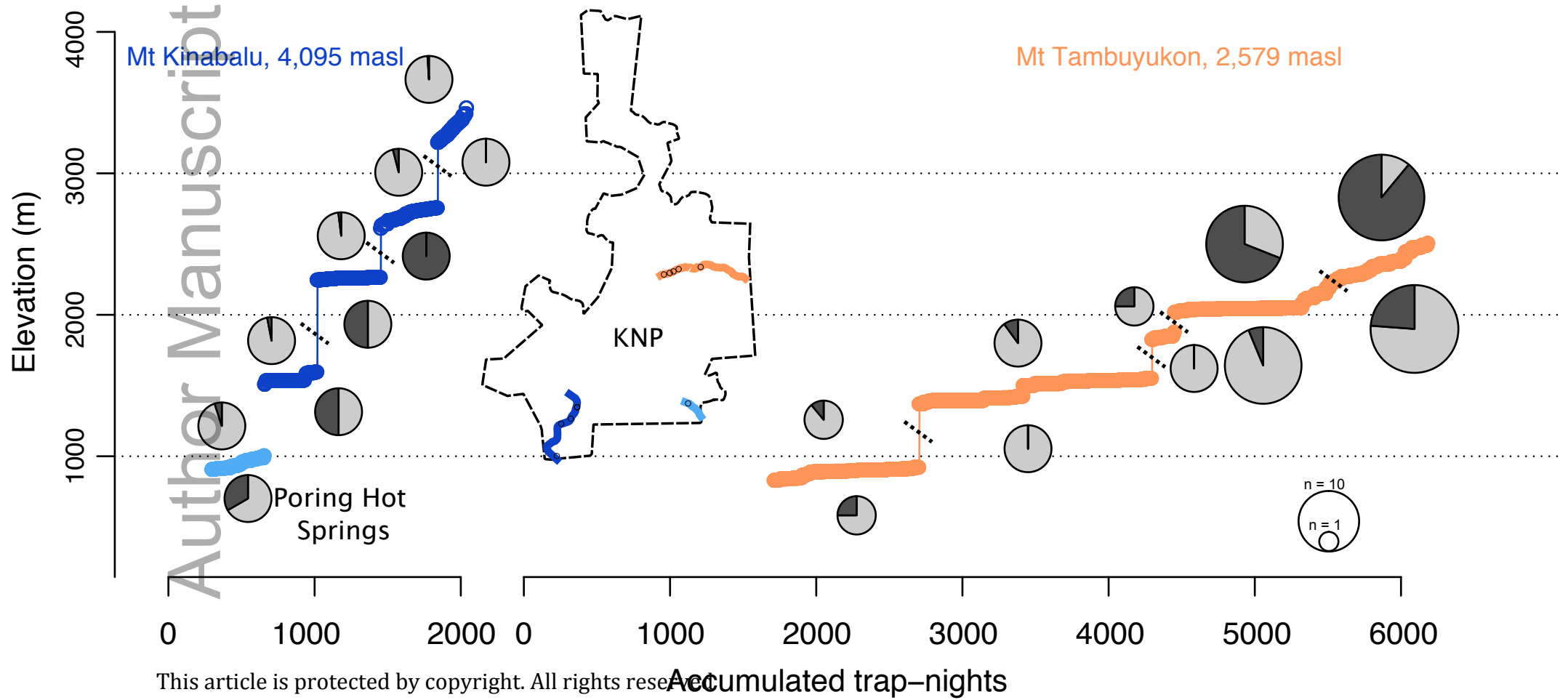
mec_15626_f2.tiff

Author Manuscript

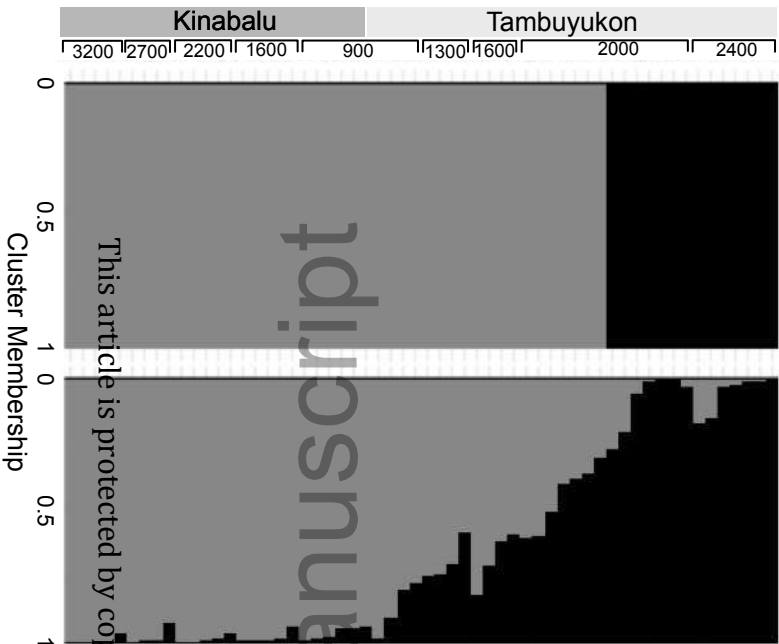


mec_15626_f3.jpg

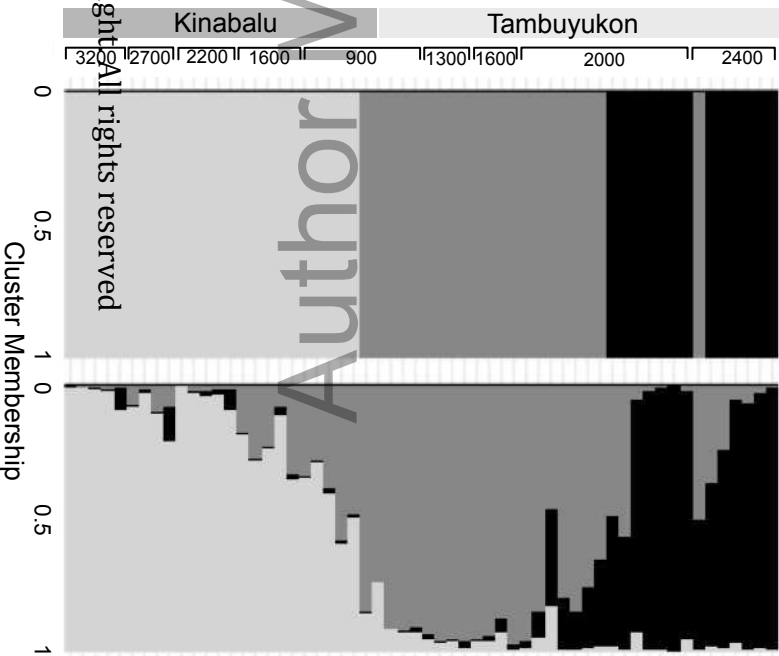
Author Manuscript

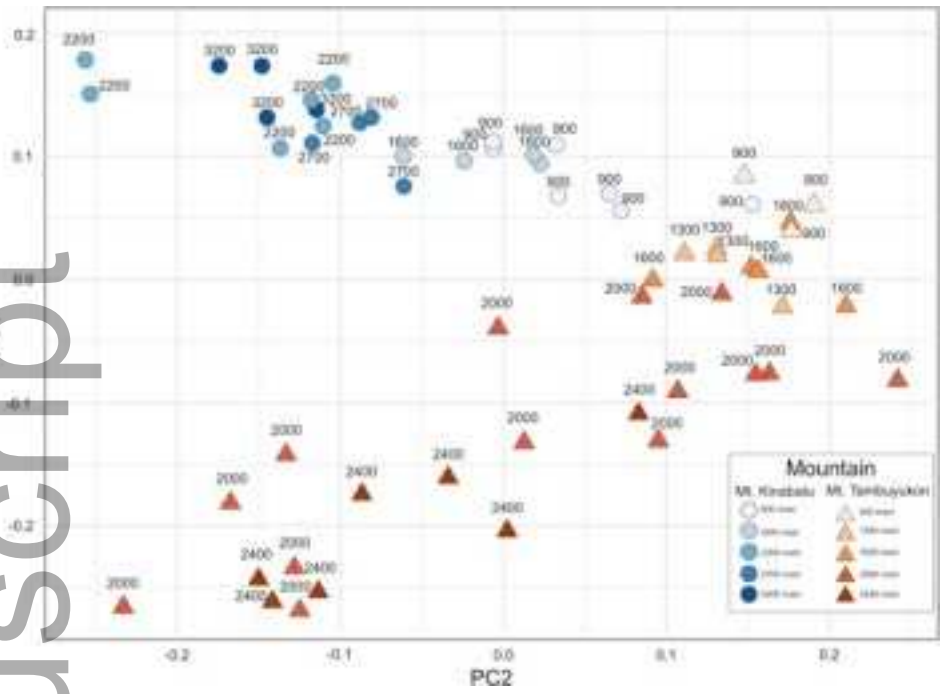


a)



b)





mec_15626_f6.tiff